ALMA MATER STUDIORUM - UNIVERSITÀ DI BOLOGNA

SCUOLA DI INGEGNERIA E ARCHITETTURA

DIPARTIMENTO DI INGEGNERIA CIVILE, AMBIENTALE E DEI MATERIALI

CORSO DI LAUREA IN INGEGNERIA PER L'AMBIENTE E IL TERRITORIO

TESI DI LAUREA

in
Modellistica Idrologica

GROUNDWATER RECHARGE ESTIMATION IN A DATA SPARSE ARID CATCHMENT OF WESTBANK

STIMA DELLA RICARICA DELLE FALDE ACQUIFERE IN BACINI ARIDI E CARENTI DI OSSERVAZIONI IDROMETRICHE: IL DARGA IN CISGIORDANIA

CANDIDATO
Alessandro Gigliotti

RELATORE:
Chiar.mo Prof.
Attilio Castellarin

CORRELATORE:
Chiar.mo Prof.
Ralf Merz

Anno Accademico 2012/13

Sessione II

Index

SOMMARIO ESTESO

Il seguente elaborato è frutto del lavoro di ricerca, della durata di cinque mesi, svolto presso il *Department of Catchment Hydrology* del centro di ricerca UFZ (Helmholtz-Zentrum für Umweltforschung) con sede in Halle an der Saale, Germania. L'obiettivo della Tesi è la stima della ricarica della falda acquifera in un bacino idrografico sprovvisto di serie di osservazioni idrometriche di lunghezza significativa e caratterizzato da clima arido. Il lavoro di Tesi è stato svolto utilizzando un modello afflussi-deflussi concettualmente basato e spazialmente distribuito. La modellistica idrologica in regioni aride è un tema a cui la comunità scientifica sta dedicando numerosi sforzi di ricerca, presentando infatti ancora numerosi problemi aperti dal punto di vista tecnico-scientifico, ed è di primaria importanza per il sostentamento delle popolazioni che vi abitano. Le condizioni climatiche in queste regioni fanno sì che la falda acquifera superficiale sia la principale fonte di approvvigionamento; una stima affidabile della sua ricarica, nel tempo e nello spazio, permette un corretta gestione delle risorse idriche, senza la quale il fabbisogno idrico di queste popolazioni non potrebbe essere soddisfatto.

L'area oggetto di studio è il bacino idrografico Darga, una striscia di terra di circa 74 km^2, situata in Cisgiordania, la cui sezione di chiusura si trova a circa 4 kilometri dalla costa del Mar Morto, mentre lo spartiacque a monte, ubicato a Nord-ovest, dista circa 3 kilometri dalla città di Gerusalemme (figura 1).

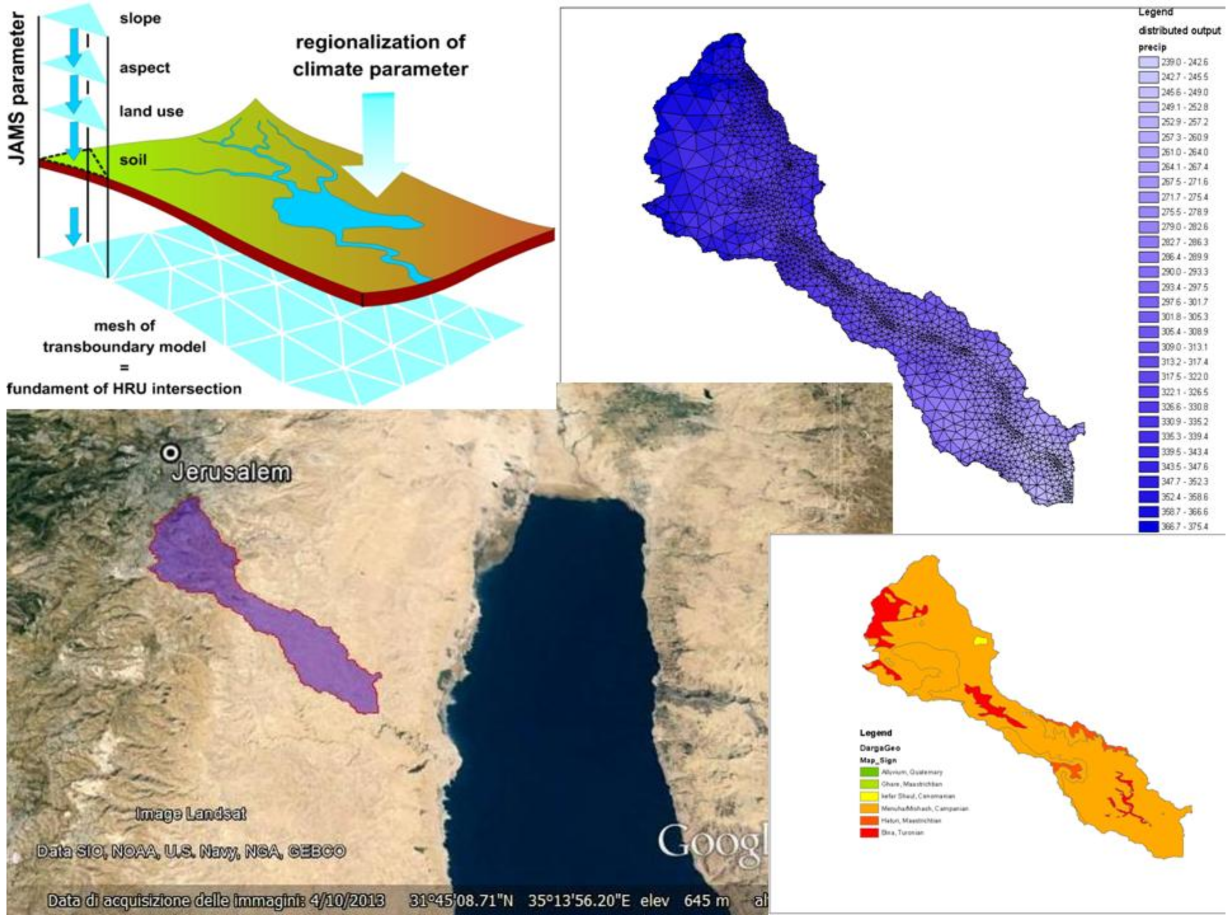

Figure 1.(partendo in basso a sinistra e muovendoci in senso orario) Ubicazione del bacino idrografico Darga. Illustrazione del metodo della discretizzazione dello spazio in HRU (unità di risposta idrologica). Assegnazione di valori medi annuali di precipitazione per ogni HRU. Caratterizzazione geologica del bacino.

La prima parte del lavoro si è incentrata sullo studio del bacino idrografico dal punto di vista climatico e geomorfologico, al fine di individuare e collezionare tutti i dati geomorfologici e climatici necessari alla modellazione numerica. La zona in esame è caratterizzata da condizioni di clima arido, con alte temperature medie annuali (25°C) e valori di evapotraspirazione potenziale giornaliera (7.39 mm) di molto superiori a quelli di precipitazione (0,86 mm). La distribuzione degli eventi di pioggia si organizza in brevi ed intensi temporali alternati a lunghi periodi di tempo secco; inoltre, va sottolineato come il bacino in esame sia assai carente in termini di misure idrometriche. Tali problematiche hanno reso la modellazione idrologica di quest’area una sfida particolarmente impegnativa poiché si sommano le difficoltà legate alla studio idrologico di un area carente di acqua a quelle legate all'utilizzo di un modello in un area carente di misure. La classica procedura di calibrazione-validazione di un modello matematico di trasformazione afflussi-deflussi, effettuata confrontando la curva delle portate osservate con quella simulata dal modello, non è percorribile nel caso in esame, disponendo per il bacino di sole misure di portata sporadica (42 giorni su di un arco temporale di 10 anni).

Lo studio ha permesso di implementare una strategia di calibrazione alternativa, chiamata *"multi-response calibration".* Tale strategia è basata sull'utilizzo di differenti variabili misurate localmente ed in remoto (da satellite) con l'obiettivo di ottenere con un unico set di parametri del modello matematico una riproduzione accurata di un insieme di osservazioni di variabili idrologiche di diversa natura simulate dal modello. In particolare, la procedura si è concentrata sulla corretta riproduzione da parte del modello dell'evapotraspirazione potenziale ed effettiva, dell'umidità del suolo e della ricarica della falda acquifera. Su quest'ultima variabile è stata posta un'attenzione particolare, essendo la sua stima affidabile il fine ultimo di questo lavoro di modellazione idrologica. Al fine di ridurre il più possibile errori ed incertezze necessariamente legati ad una procedura di calibrazione-validazione non convenzionale, sono stati utilizzati due differenti metodi di calcolo della ricarica della falda acquifera, uno in calibrazione e uno in validazione. Durante la fase di calibrazione è stata utilizzata l'equazione di *"Guttman and Zukerman"*, calibrata per le aree aride e già utilizzata con successo in Medio Oriente (Guttman & Zukerman, 1995). Detta procedura lega la ricarica della falda acquifera al valore della precipitazione tenendo conto dell'intensità dell'evento. Per la fase di validazione si è invece utilizzato un metodo ancora più preciso, che è il bilancio di massa del cloruro; la ricarica della falda acquifera è stata stimata in funzione della pioggia e della concentrazione di cloruro contenuta nelle acque piovane e in quelle sotterranee. La precisione del metodo e il suo basarsi su dati raccolti in campo ne determinano un'affidabilità comparabile a quella di osservazioni dirette dei movimenti della falda acquifera. La bontà del modello nel simulare andamenti delle variabili di interesse comparabili a quelli reali è stata misurata utilizzando diverse funzioni obiettivo (ad es. efficienza di Nash -o coefficiente di determinazione-, R^2, Errore Medio Relativo).

La struttura della Tesi ricalca fedelmente le fasi in cui il lavoro di ricerca è stato suddiviso, articolandosi in 10 capitoli:

- Il primo capitolo è un introduzione al problema del sostentamento del fabbisogno idrico in Cisgiordania; vengono descritti gli scopi del progetto, gli strumenti che sono stati utilizzati e le problematiche incontrate.
- Il secondo capitolo espone i concetti teorici di base e le definizioni fondamentali della modellistica idrologica, elementi funzionali alla comprensione dell'elaborato.
- Il terzo capitolo è un analisi approfondita e dettagliata del bacino idrografico in esame. L'area viene descritta dal punto di vista climatico, geologico e pedologico con particolare attenzione alle caratteristiche che influenzano il processo idrologico.
- Il quarto capitolo contiene la descrizione del modello idrologico spazialmente distribuito a base concettuale utilizzato nello studio, J2000g ottenuto come semplificazione del modello più complesso J2000 (Krause, 2009), ne viene descritta la struttura, il significato dei parametri che governano il calcolo delle variabili e gli output che genera.
- Il quinto capitolo descrive il processo di raccolta e sistematizzazione degli input necessari a far girare il modello, esso descrive le fonti da cui i dati provengono e la loro natura, da quelli di tipo climatico a quelli legati a topografia, pedologia, idro-geologia e uso del suolo.
- Il sesto capitolo fornisce la descrizione del lavoro svolto in ambiente GIS per effettuare l'analisi idrologica dell'area in esame ed estrarre lo spartiacque del bacino idrografico partendo dalla conoscenza della posizione della sezione di chiusura del bacino stesso e da un modello digitale delle quote del terreno della regione in esame.
- Il settimo capitolo riguarda la fase di calibrazione del modello, viene illustrata la strategia alternativa di calibrazione utilizzata nello studio.
- L'ottavo capitolo descrive la fase di validazione del modello e la valutazione dell'efficienza, in particolar modo si concentra sulle variabili di confronto utilizzate nella strategia di validazione e sulle funzioni obiettivo considerate per valutare l'affidabilità predittiva del modello.
- Il nono capitolo riporta una descrizione dei risultati ottenuti, vengono mostrati e commentati gli output spazialmente distribuiti delle variabili di interesse.

- Il decimo capitolo si concentra sulle conclusioni del lavoro, vengono discussi i risultati ottenuti e proposti miglioramenti tecnici.
- L'ultima parte dell'elaborato è un appendice contenente la lista degli script creati in Matlab per portare a termine le fasi di calibrazione, validazione e valutazione della bontà del modello.

1. INTRODUCTION

A wise water resource management is of high importance in areas characterized by water shortage, where water is an extremely valuable resource, and cannot be wasted. According to the Palestinian water Authority the quantity of water used for domestic purpose in West Bank in 2003 was 64.7×10^6 m^3, which averaged over a population of 2,313,609 (Marei et al., 2010) means roughly 86 l per person without considering the water losses associated with water transportation, which suggests that the true value is probably significantly lower. If one compares this value with the amount of water recommended by the World Health Organization, 150 l per person, he/she can easily understand why water resource management is so important in this area of the world. Moreover, in addition to the water shortage, a large number of Palestinian communities are not connected to the water supply systems networks. Groundwater is actually the most important source of fresh water in the area.

The main aim of this Dissertation is trying to make a reliable estimation of groundwater recharge in an arid catchment of Israel, which is ungauged in the sense that no direct runoff measurements are available for the study catchment. Some of the most used and well established techniques to extract useful information from areas with lack of data are presented herein, and the dissertation also present a general discussion on some of the most problematic situations hydrologists have to face in cases like this.

The present study considers a conceptual spatially distributed hydrological model, working at a daily temporal resolution. Input data comes from local authorities, previous field inspections and, where missing, literature values. The study shows that the model *J2000g*, under an appropriate parameterization, is able to describe at daily time step the replenishment of the aquifer along with other hydrological variables such as actual evapotranspiration, soil moisture, etc.. The goodness of the model's performance is assessed by comparing the distributed variables with the corresponding measured or theoretical (i.e. expected) values, where possible, and by performing an analysis of precision and efficiency. All the information about the basin such as soil properties, geology, land cover and topography are managed and analyzed within a GIS (*Geographical Information System*) environment (ArcGIS® software), while Matlab® scripts were specifically written for plotting results and calculating efficiency factors. The scripts are attached and commented in an Appendix.

Estimation of groundwater recharge in this area is a challenging goal because we had to face the sum of three different problems:

- Implementation of hydrological modeling in arid and semi-arid areas, where precipitation is absent in most part of the year and it occurs only in few short and very intense events with the form of thunderstorm.
- Predictions in ungauged basins: the almost total absence of runoff data leads to the impossibility to apply a normal calibration-validation strategy, based on comparing simulated runoff with observed series. Another strategy for calibrating and validating the model, based on a multi-response comparison of different hydrological variables, was identified and used.
- Information comes from different sources and several data are affected by large uncertainty and measurement errors (e.g. daily temperature values from Israeli meteorological service, IMS).

This study borders some of the most difficult, and still open, problems of hydrology and, thanks to some necessary assumptions and simplifications, demonstrates the possibility to make reliable predictions and extract useful information from and for this area.

2. CONCEPTS OF HYDROLOGICAL MODELING

2.1 Hydrological Variables and Models

2.1.1 Basic concepts

Hydrology is the study of hydrologic cycle, water resources and environmental watershed sustainability on the Earth. Qualitatively the hydrological cycle at Earth scale is composed by the following main phenomena (figure 2.1):

- Precipitation: can be liquid or solid, it has high variability in time and space.
- Interception: amount of water that does not reach the soil, but is instead intercepted by the leaves and branches of plants and directly evaporates from them.
- Evaporation: water vapor that returns from the surface again to the atmosphere
- Transpiration: water vapor that returns the atmosphere due to plants life-cycle
- Infiltration: amount of water that reaches the soil and penetrate it due to gravity and capillarity forces. It doesn’t become surface flow.
- Percolation: is the infiltration in the deeper layers, in permeable rocks, until reach groundwater storage.
- Surface runoff: amount of water that flows in the surface.

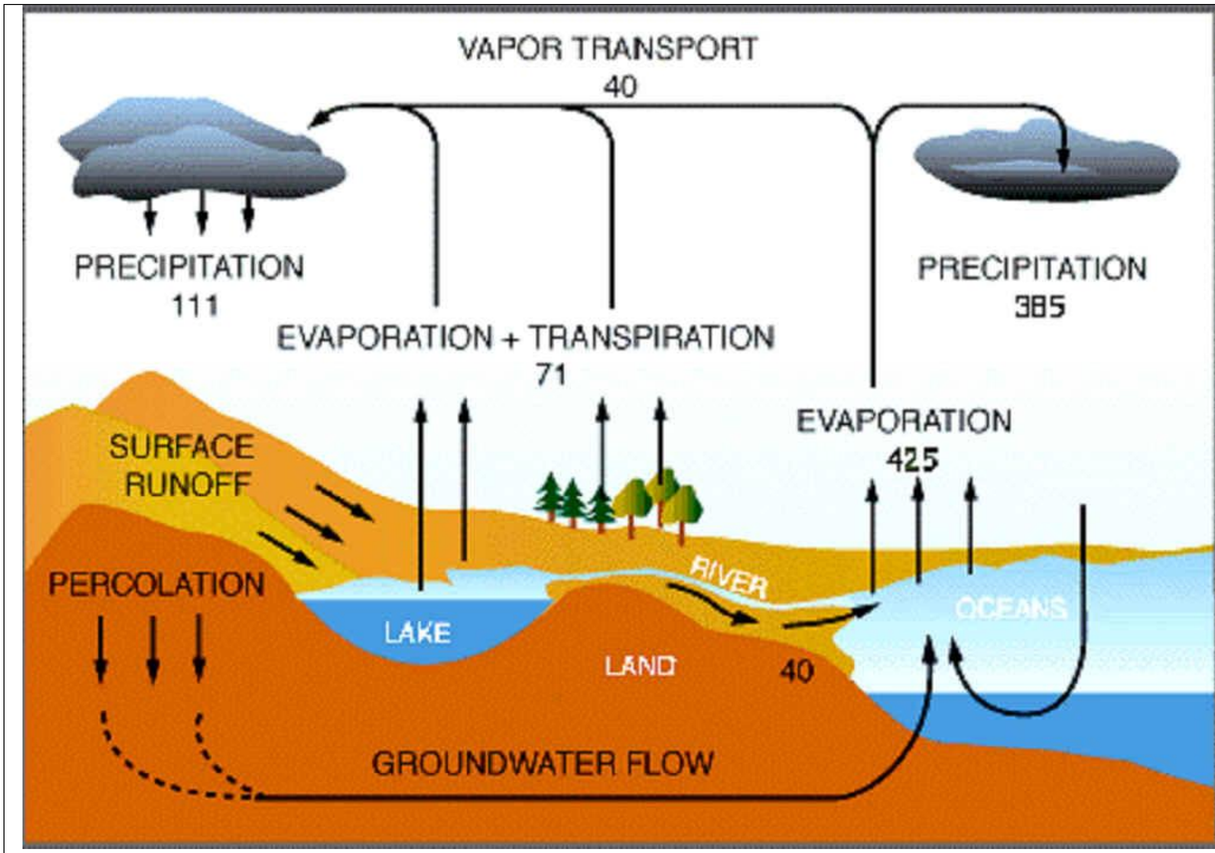

Figure 2.1 Hydrological cycle, Values in 10^3 km^3/yr (http://www.globalchange.umich.edu).

A hydrological model is a system of mathematical equations with the aim of simulates part of the hydrologic cycle. It is used to calculate one, or more, hydrological variables. A hydrological variable is a real (or integer) number characterizing a physically observable quantity in a hydrological process. Although it is a deterministic quantity it is usually described stochastically because lot of hydrological phenomenon are not perfectly known or we do not have the instruments to described them mathematically.

A model is characterized by input variable, output variable, state variable and parameters:

- Input variable: what we introduce in the model, known data about the phenomenon from which depends the quantity we want to estimate,
- Output variable: what we want the model to calculate; it is the quantity we want to estimate,
- State variable: characterize the mathematical state of a dynamic system,

- Parameters: describe proprieties of the system, can be constant or vary in function of time.

Equations of the model basically describe exchanges of water volumes under two principles from fluid mechanics:

- Conservation of mass;
- Conservation of energy.

2.1.2 Classification of hydrological models

Application of Hydrological models has three main purposes: Calibration, Prediction and Solution of Inverse Problems.

- Calibration: we have knowledge of input and output variables and we want to find the best parameter set.
- Prediction: that is the most common purpose for which models have been developed, we know input and parameters and we want to estimate the output variables.
- Solution of Inverse problems: quite rare in hydrology, it refers to the cases in which there is knowledge of parameters and output and the aim is to calculate the input.

Models can be deterministic or stochastic: they are defined as deterministic when at one input correspond always the same output, there are not stochastic processes in the calculations of the output variables. Otherwise they are stochastic if at least one of the variables of the models is governed by a stochastic process, which means the result can change also when the input are the same. As said before this “trick” is used in hydrology to pay the not perfectly knowledge we have about some of hydrologic phenomenon.

Models can also be classified according to their structure, work scale and characteristic of simulation. Regarding structure models can be:

- Physically based: the equations try to describe mathematically the real dynamic of the natural phenomenon. As hydrological phenomena have always spatially variability, physically based models have to be spatially distributed.

- Conceptually based: take in account the real dynamic of the phenomenon but make some assumptions and simplifications.
- Black box: equations have nothing to do with the real dynamic of the phenomenon; the only aim is to give realistic output.

Concerning spatial scale models can be:

- Lumped: models work considering the entire basin as a unique spatial unit; variables depend on the time but not on the space.
- Distributed: models divide the basin in spatial units which can be considered homogeneous for hydrologic characteristics; variables depend on both time and space.
- Semi-distributed: models work in sub-basin scale, so each calculation is made for every sub-basin and then the results are propagated to the outlet.

A basin is a topographic area, identified by a close polygon termed watershed, where all the rain falling in the area flows in only one point, which is the outlet of the catchment.

Regarding characteristic of simulation models can operate continuously in time, or be event-based (i.e. reproducing single event). Models which are good in modeling events (e.g. extreme events) are usually not good in the continuous simulation, and models accurate in the continuous prediction usually are not able to well simulate extreme events.

2.1.3 Calibration and validation

In most of the cases it is not possible to directly measure the parameters of the model or to identify reliable parameter values in the literature, usually parameters values have to be adjusted to better fit with observed values. As already mentioned, the process to find the best parameter set is called calibration (figure 2.2). Calibration need the knowledge of input and output data, in the same time step and for the same time period. Model parameters are changed (manually or by using automatic algorithms that minimize or maximize mathematical objective functions) in order to make the output of the model as close as possible to the observations. With the assumption that what happens in the past can guide us in the prediction of what will happen in the future, we suppose that the parameter set found to be the best for the observation period will also be good for the near future, if general conditions in the catchment do not change significantly.

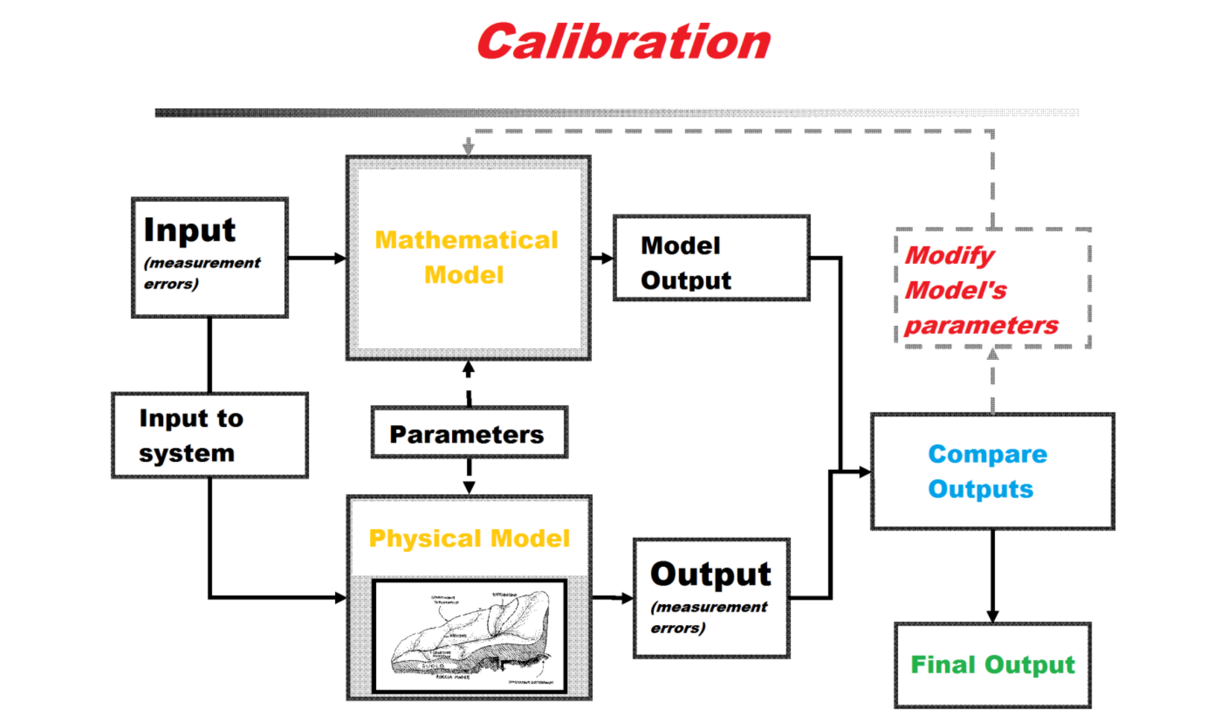

Figure 2.2 Calibration strategy. (Montanari & Castellarin, 2013)

Once identified a suitable parameter set through calibration we have to validate the model, which means check the goodness of its prediction. For this purpose we need another set of data complete of input and measured output, which should be different from the one used during the calibration. Validation ends with comparing the model output with the real one; if the simulated series fit with the measured ones the model is able to make reliable prediction in the catchment.

2.2 Predictions in ungauged basins

Simulation is always subject to uncertainty, mostly because a model does not reflect perfectly the reality and the data available can contain errors. When measured data for calibration-validation are missing, or are sparse and insufficient, uncertainty increases because the goodness of model output cannot be checked properly. Under these circumstances a different strategy for calibration-validation has to be found. This is the case of prediction in ungauged basins (PUB).

An ungauged basin is a catchment with inadequate records (Sivapalan et al., 2010), the inadequacy can be in terms of quantity or quality of the data and it makes impossible to calculate the variables of interest in the appropriate spatial and temporal scale and with acceptable accuracy for practical applications. For example if the variable of interest has not been measured for the required time period, or with the wrong resolution the basin would be classified as ungauged with respect to this variable.

In fact, in order to make certain predictions, Hydrological modeling always requires the proper identification of three main components:

- A model that can describe hydrological processes,
- A set of parameters that describe the basin's proprieties that mainly drive the processes we want to study,
- An appropriate meteorological input.

These components can be not all perfectly known or, in the worst case, not known at all because of the space and time heterogeneity. A prediction in ungauged basin is the prediction, and its associated uncertainty, without using the past time series of the variable that is being predicted, so without the possibility to make a direct calibration. Also validation, comparing results with observed data, is not possible and that means predictions in these cases cannot be verified with confidence, so they are always affected by uncertainty. The uncertainty in the prediction does not come only from lack of validation, but also from the process of prediction due to lacks in its components. That is because there is heterogeneity in the climate variable, in the landscape and in the dynamic of processes, which cannot be perfectly described by the prediction system. There are three kinds of uncertainty:

- Uncertainty in model structure (i.e. the model cannot correctly reproduce the landscape space)
- Uncertainty in model parameters

- Uncertainty in climatic input

The prediction in ungauged basin is generally most focused on water quantity and availability problems (flood flows associated with a given exceedance probability, soil moisture, groundwater recharge, low-flow variability, etc.) because water quality problems need the knowledge of the flow partitioning to be solved. We also focus on quantitative aspects of the water cycle in the basin, as our goal is to predict the groundwater recharge continuously in time and distributedly in space.

3. DESCRIPTION OF THE STUDY AREA

The West Bank is a territory located in Western Asia. It is geographically included in the state of Israel, meaning that West Bank shares boundaries with the state of Israel to the West, North, and South, while to the East, across the Jordan River, it shares boundaries with Jordan and part of the west Dead Sea coastline. Regarding similitude in climate, hydrogeological characteristics and land cover West Bank can be divided in three parts: Western, Eastern and Northeastern. Focusing on groundwater movement in the mountain area, three groundwater basins were identified; one in each zone (Marei et al., 2010). The Dead Sea has an elevation of 410 m below the sea level and is the lowest part of West Bank.

The Darga catchment, which is the study basins, is a strip of land of 73.926.900 m^2, situated in the Eastern part. Its outlet is situated at about 4 km from the Dead Sea shoreline and the higher part of the catchment is situated 3 km far from the city of Jerusalem (figure 3.1). Its elevation ranges between 809 meters above the sea level in the north-west of the catchment and 15 m below the sea level in the south-east part, in correspondence of the outlet (figure 3.2).

Figure 3.1. Position of Darga catchment.

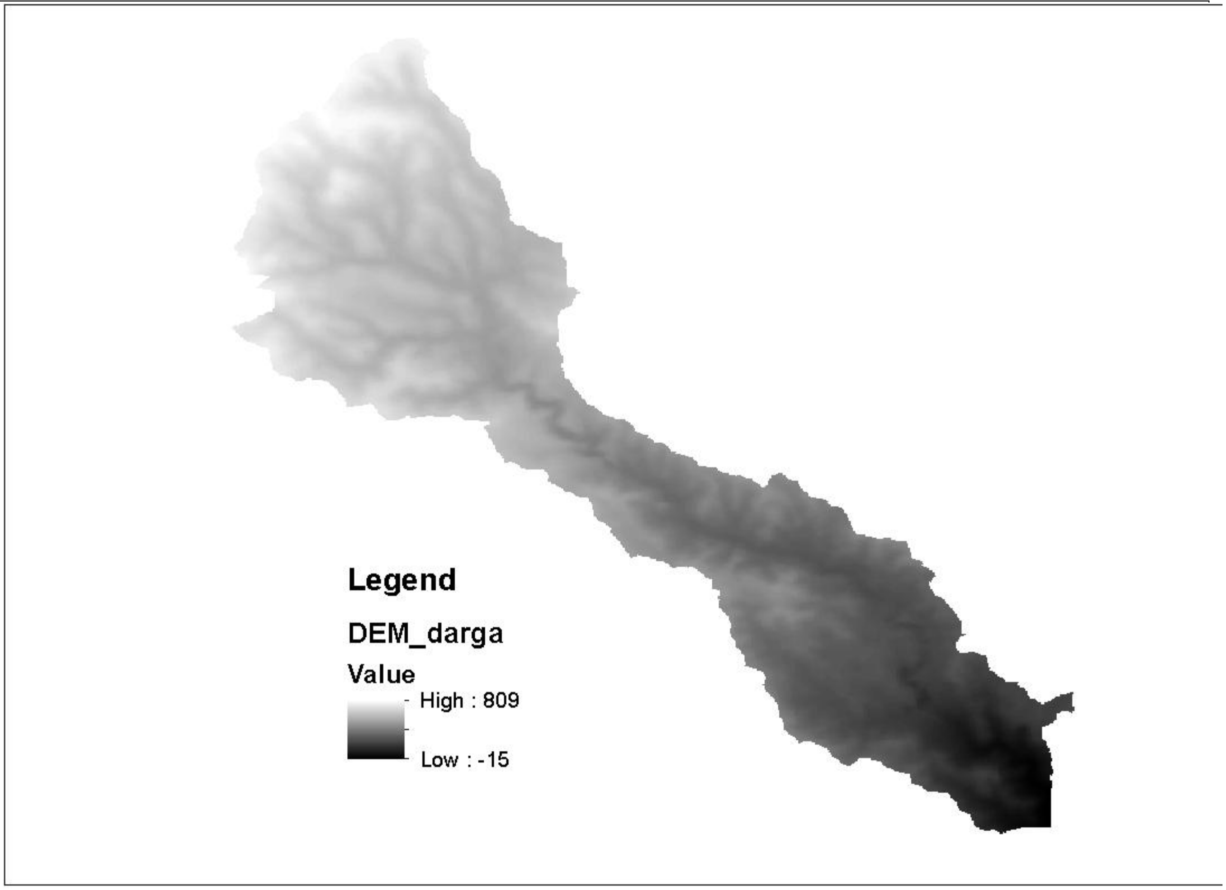

Figure 3.2. Digital elevation model (DEM) of Darga catchment.

3.1 Climate:

The climate in West Bank is mostly controlled by three factors: the distance from the sea, the distance from the deserts and the elevation from sea level. The Mediterranean Sea influences the humidity, the fluctuation of temperature and the amount of rainfall. Near the deserts humidity decreases, mean temperature (daily and seasonal) increases and precipitation decreases. Elevation affects the climate by increase rainfall and decrease humidity; mean temperature also decrease with elevation.

The climate change from semi-humid in the western side to the arid in the eastern, in fact precipitation is above 600 mm/year on the mountain ridge and below 100 mm/year on the Dead Sea Shore (Palestinian Water Authority). The rain events occur mostly during the winter and spring seasons, and during events of high intensity, i.e. more than 50 mm per day or more than 70 mm in two days (Raffety, 1965), surface runoff is observed.

August is the warmest month of the year and the mean temperature can reach 34°C along the Dead Sea shore. January is the coldest month and the mean temperature is around 16°C near the Dead Sea but far from it, in the western part, can also go below 10°C.

Darga catchment is situated in the eastern zone and reflects this trend. Precipitation is higher in the west part (that is also the upper part), almost linearly decreases in the east part and has a minimum near the Dead Sea shore. Annual precipitation ranges between 200 and almost 400 millimeters, it has a high variability in space and time.

Climate condition of the catchment can be described as arid. In reality it is difficult to derive a unique and practical definition of arid environments because they are extremely diverse in terms of land forms, soils, fauna, flora, water balance and human activities (The Food and Agriculture Organization of the United Nations, 1989). Usually aridity is expressed as function of precipitation and potential evapotranspiration, one of the most used indexes is the climatic aridity index: P/PET, where P is precipitation and PET is potential evapotranspiration calculated by the method of Penman. Depending of the value of these index arid areas can be divided in three categories:

- Hyper arid zone: arid index 0.03 or lower. Usually they are dryland areas without vegetation, with the exception of few shrubs. Annual rainfall is low, usually not higher than 100 millimeters, and it occurs in irregular and infrequent way. Often there are period, also longer than year, without rain and after short period of intense precipitation with the form of thunderstorm.
- Arid zone: arid index ranges between 0.03 and 0.20. It is characterized by sparse native vegetation, usually shrubs, herbaceous and small threes; the presence of farm is possible only if artificial irrigation is available. Precipitation is characterized by high variability, with annual sum ranging between 100 and 300 millimeters.
- Semi-arid zone: arid index between 0.20 and 0.50. Native vegetation is quite various, with lot of species. Annual precipitation varies a lot depending on the season: in winter it range between 200 to 500 millimeters and in summer between 300 and 800.

Rain is enough to support agriculture with not too high level of production without the help of artificial irrigation.

- Sub-humid zone: arid index between 0.50-0.75. It is not a properly humid zone so it is also classified in the term “arid zone” because in it is possible to find condition typical of arid climate.

Darga catchment has an average daily PET of 7.39 mm and an average daily rain of 0.86 mm, the value of aridity index is 0.12 which means it is an arid area. Values of annual precipitation also confirm that, because they range between 200 and less than 400 mm and the precipitation occurs mostly in winter moths with short intense thunderstorms spaced by long periods of completely dry conditions.

3.2 Geology

Eastern part of Israel is characterized by erosive activity, increased by the difference between the elevation of Dead Sea and the Mediterranean Sea (Arieh Singer, 2007). There are five aquifers within the Eastern basin. The main one is the Judea Group aquifer, which consists of limestone and dolostone of Early Cenomanian to Turonian age. The secondary aquifers consist of limestone and chalk of Eocene age in the Samaria syncline, basalt of Neogene-Quaternary age in the lower Galilee area, alluvium fill of Neogene-Quaternary age in the Bet She'an area and the Jordan Valley, and limestone of Jurassic age. (Geological survey of Israel)

Darga Geology is characterized by sparse formations of Limestone, marl and dolostone from the Turonian age (“Bina” in figure 3.3) but most part of the geological formation is composed of a mixture of Menuha and Mishash from Upper Cretaceous age (figure 3.3). Mishash is mostly composed of chalk, phosphorite, massive chert and fossiliferous limestones. Menuha is composed of dolomite, bitumen, phosphor, silty chalk and chert. Percent of the composition can vary in function of the geographical location.

Every geological unit has hydraulic proprieties which influence qualitatively and quantitatively the dynamic of groundwater recharge in the catchment. Mishash is rather permeable, so it has the proprieties of an aquifer, where aquifer is defined as a layer of permeable rock or unconsolidated materials from which groundwater can be extracted.

Menuha has low permeability so it is defined as having the proprieties of an aquitard. Bina is the name of a geological formation really common in Israel characterized by high permeability; it can be divided in Deronim, Shivta and Nezer formations (Dan, 2001).

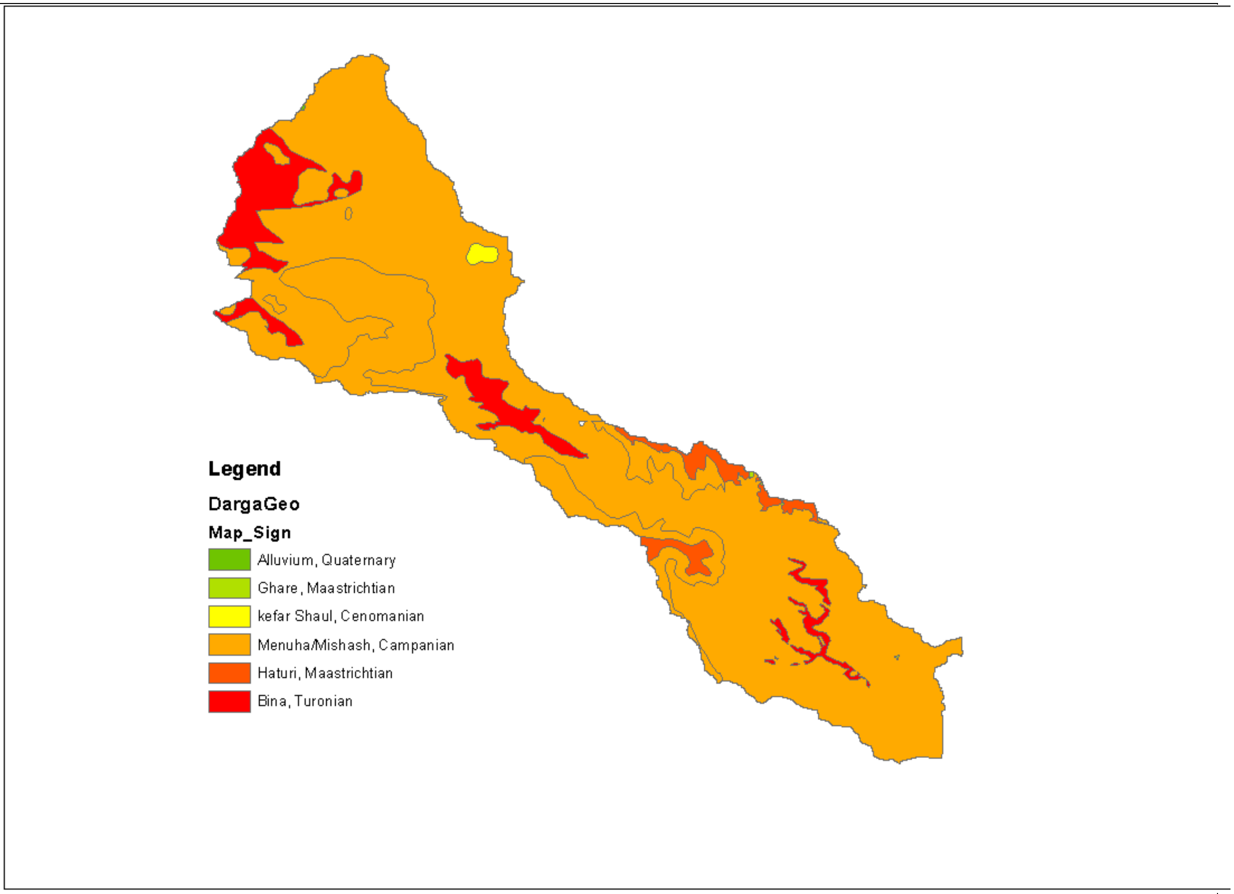

Figure 3.3. Geological units in Darga catchment.

3.3 Soils

Soil distribution in Israel generally follows lithology and topography. Here is presented a short description of the soils of Darga catchment; however the area is not really big there is a difference between north and south. Soils influence also hydraulic characteristics of the catchment, that is why it is important to know which soil type can be observed in each part of the basin. The difference in presence of soils also reflects the difference of climate conditions, in fact in the Northern portion of the catchment can be found soils which usually occur in semi-humid or humid conditions, otherwise in the south there is presence of soils typical of arid conditions. All the soil types will be described focusing on composition, conditions in which occur, classification in two different systems, USDA and FAO, color (in order to be able to recognize them in field) and hydraulic proprieties. Particular attention is given to the content of clay, sand and silt of every soil type which highly influences hydraulic characteristics such as porosity and hydraulic conductivity. So it’s useful to remember that:

- Clay: $d < 0{,}002$ cm,
- Silt: $0{,}002$ cm $< d < 0{,}05$ cm,
- Fine Sand: $0{,}05$ cm $< d < 0{,}25$ cm,
- Coarse Sand: $0{,}25$ cm $< d < 2$ cm,

Where d is the grain size (diameter).

The USDA Soil Classification is an elaborate classification of soil types developed by United States Department of Agriculture and the National Cooperative Soil Survey that groups soils in several levels according to their properties.

FAO soil classification is a supra-national classification, also called World Soil Classification, developed by The Food and Agriculture Organization of the United Nations (FAO) which offers useful generalizations about soils pedogenesis in relation to the interactions with the main soil-forming factors. Many of the names used in this classification are known in many countries and do have similar meanings worldwide.

An average value of bulk density is estimated for this area by the World Soil Classification, and it is 1.49 kg/dm^3; bulk density is a really important parameter to take in account in some compaction process, usually involving vibration of the container, and it is defined as the mass of many particles of the material divided by the total volume they occupy. The total volume includes particle volume, inter-particle void volume, and internal pore volume. Bulk density is not an intrinsic property of a material; it can change depending on how the material is handled.

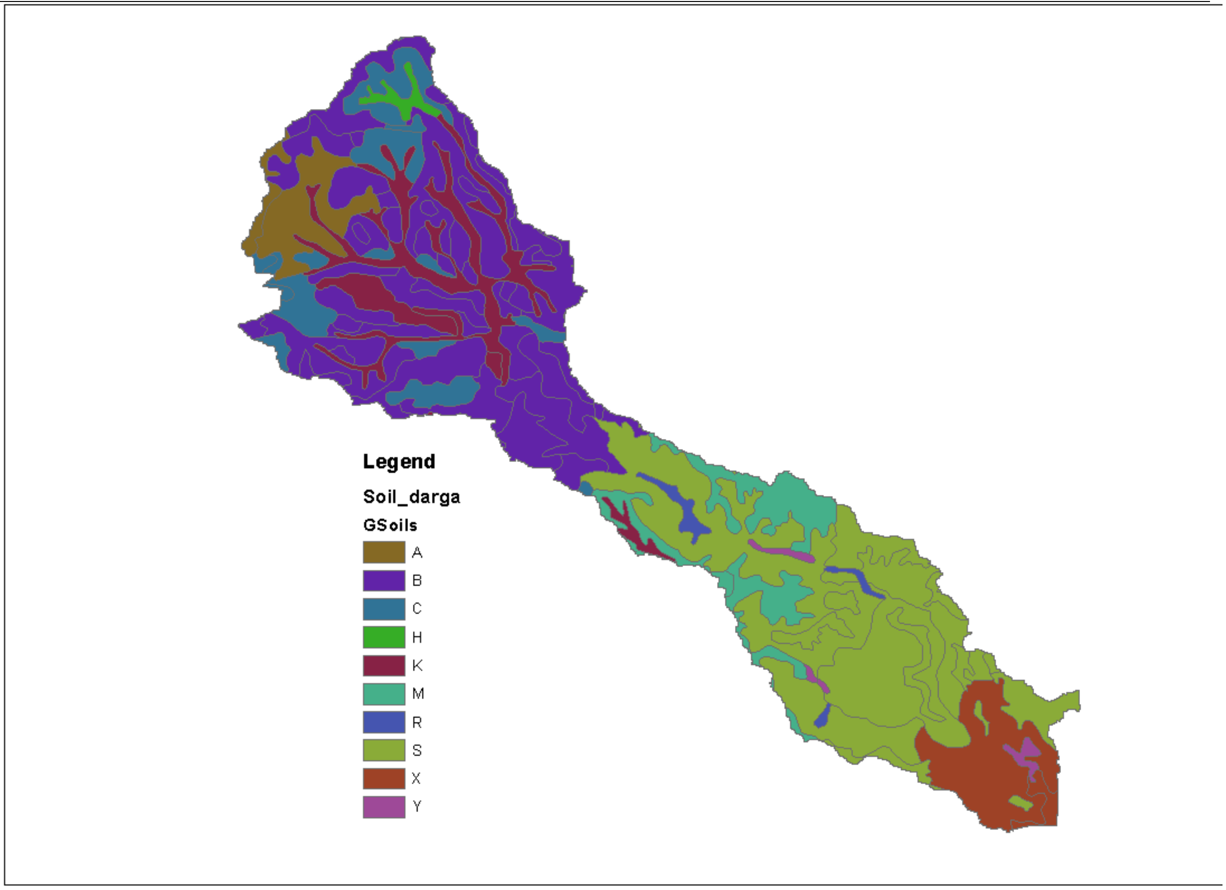

Figure 3.4. Soils of Darga catchment. Letters represent the following soil types: Terra Rossa (A), Brown Rendzina (B), Pale rendzina (C), Vertisol non saline on alluvium (H-K), Light Brown Sandy Loam (M), Loess Serozem (R-S), Reg Soil (X-Y).

3.3.1 Soils in North of Darga catchment

As said before, distribution of soils, as it occurs for geology, change a lot between north and south. North of Darga catchment is characterized by Terra Rossa, Brown Rendzina and Pale Rendzina (letters A, B and C of figure3.4). The first one is present in limestone and dolomite; Rendzina soils are found mostly on chalk and marl. There is also a sparse presence of Vertisol non saline, on alluvium. (H and K in figure 3.4)

In the USDA soil classification, Terra Rossa would be classified as Rhodoxeralf or Haploxeroll, in the FAO classification as Luvisol. Rendzina in the USDA classification would be classified as Haploxeroll or Xerorthent and in the FAO classification as Rendzina (Arieh Singer, 2007).

TERRA ROSSA

Terra rossa is usually found in continuous extended layer, however it is more common in humid climate it can be observed also in arid areas, but with some of its proprieties changed. It is composed by dolomite and limestone from the Turonian age with some calcareous sediment. Its formation is due to the exposition of these rocks to Mediterranean conditions. Soil depth in this area can reach 60 cm and the color varies from brown of the upper horizons to red and dark red in the deeper layers. The content of clay is usually really higher than the content of sand and it increase with the depth; It is always more than 60%, sand is around 10% and the rest is silt. Field capacity is moderate.

PALE RENDZINA

Rendzina soils are rarely continuous and usually mixed with other soil type; in the north of Darga basin they are mixed with Vertisol, which is a colluvial soil, but it is not uncommon to observe Rendzina soils in association with Terra Rossa. Usually Rendzina soils occur on pour calcareous sediments, mainly chalk and marl. As same for Terra Rossa this kind of soils are mostly present in humid climate conditions but a particular soil of the group, Xerorendzina, is found also in arid and semi-arid conditions. The composition can vary but usually it includes high content of $CaCO_3$ and clay minerals. Depth is moderate: for Pale Rendzina (Xerorthent in the USDA soil classification) it cannot reach more than 80 cm. the clay content is lower respect to Terra Rossa, around 55%, sand content is around 20%. There are some difference between Pale Rendzina soils developed on chalk and the one developed on marl. The first group usually has lower content of clay, more carbonates and paler color, from light grey in the upper layer to white in the deepest horizon. The second group has color varying from dark grey (higher content of clay) to light yellowish brown. Hydraulic conductivity of Pale Rendzina soils is good, but it decreases when the clay content increases.

BROWN RENDZINA

Brown Rendzina (Haploxeroll in the USDA soil classification) represents an advanced stage of Rendzina soils development (Dan et al., 1972) which occurs when erosion is prevented. It comes from calcareous rocks of moderate hardness and porosity, according to Dan (1976) the formation took place in semi-arid and arid climate conditions due to the precipitation of carbonates, it is usually associated with Nari lime crust. Depth is limited, usually below 30 cm. The color varies from very dark brown to brown in the deeper layers. Clay content is about 45% and sand content between 15 and 25%, it increase with the depth. Porosity is around 35% and conductivity is good as the one of Pale Rendzina, water holding capacity is moderate.

VERTISOLS

In Israel colluvial soils covering wadi beds are not uncommon. These soils can develop on two different rock formations: fine-grained alluvium and basalt, but the formation from alluvium is more frequent (Arieh Singer, 2007). They can be found in a very large range of climate conditions, from humid to arid climate. In the Darga area can be observed few formations of Non-saline Vertisol, developed from alluvium, typical for the area characterized by arid or semi-arid conditions. For this soil the content of clay reach values of 60%, otherwise the content of sand is quite low, usually around 5%. Depth can be really high, until 150 cm and the color changes from the red-brown in the 0-12 cm horizon until the dark red-brown in the 90-150 cm horizon. Water-holding capacities are high while infiltration is low, hydraulic conductivity is also low.

3.3.2 Soils in South of Darga catchment

South part of Darga catchment is dominated by the presence of Loess Serozem and Light Brown Sandy Loam (R, S and M in figure 3.4). Near the Dead Sea shoreline, in proximity of the basin’s outlet, there is a heavy presence of Reg Soil. (X and Y in figure 3.4)

LOESSIAL SEROZEM

This soil, typical of arid areas, is composed by Aeolian sediments, according to the most accredited theory originated from desert (Reifenberg, 1947). The color varies from pale brown to yellowish brown depending on the depth, which can be very high, In fact in this area this kind of soil can reach the depth of 190 cm. the content of clay is around 20%, the content of sand 25% in average but it decrease with the depth; in the first layer the content of sand can reaches 35%. Infiltration capacity is moderate but soil moisture movement both in horizontal and vertical direction is rapid.

LIGHT BROWN SANDY LOAM

Light Brown Sandy Loam is a closed parent of Loess Serozem; it also comes from Aeolian sediments, after various sedimentation cycles. Is composed mainly by sandy sediments but include however also finer-grained materials of Loessial character. It's a soil observed mostly in arid areas; the color is very pale brown and doesn't show big variations. The depth is around 170 cm, which a content of clay that can varies from 90% in the upper layer to 70-80% in the most depth horizon. Content of clay is quite low, about 10% in average. As said for Loess Serozem, the infiltration capacity is moderate but soil moisture movement is rather rapid.

REG SOIL

Reg soils are typical of desert climate conditions, so extremely arid with rare precipitation, usually in the form of thunderstorm. These Soils are composed by limestone, dolomite, chalk, flint and marl, together with some fines materials, the content of $CaCO_3$ is usually high. The content of clay is about 20% in average but it varies a lot with the depth in a non-linear trend, the content of sand is quite high, about 40% with values that can reach 60% in the deeper horizon. The presence of well-defined soil horizons distinguished Reg soils from other desert soils; in fact it is one of the most stratified soils we can observe in this area. Its depth can reaches 170 cm. the color varies from very pale brown to reddish-yellow. Infiltration capacity is moderate.

3.4 Land cover

Vegetation is highly influenced by climate; its characterization is important because it affects the process of evapotranspiration and so the hydric balance. Vegetation cover in arid zone is scarce but some plant forms often occur in it and can be classified as:

- Ephemeral annuals, which appear after rain; their growth lasts only in a short wet period and their life usually doesn't exceed the 8 weeks. They have small size and shallow roots.
- Succulent perennials are able to accumulate and store water and participate to the process of evapotranspiration. Cacti are typical example of succulent perennials.

- Non-succulent perennials comprise the majority of plants in the arid zone. These are hardly plants including grasses, woody herbs, shrubs and trees that can hold out the unfriendly conditions of arid areas environment.

Darga catchment's land cover changes a lot between north and south, reflecting the changing of climate conditions. The lowest part, near to Dead Sea, is almost totally composed of rocks, without vegetation (figure 3.5). In the middle of the catchment can be observed an equal presence of rocks and open soil, so still the vegetation is absent or so rare that could not affect the hydric cycle. Vegetation occurs in the upper part of the catchment (figure 3.5), the one that present higher elevation and higher value of precipitation. In this part a wider variety can be observed: open soil is still highly present but together with sparse vegetation, agricultural crop, shrubs and plants characterized as deciduous forest. Also a few anthropological presences are distinguished in the map.

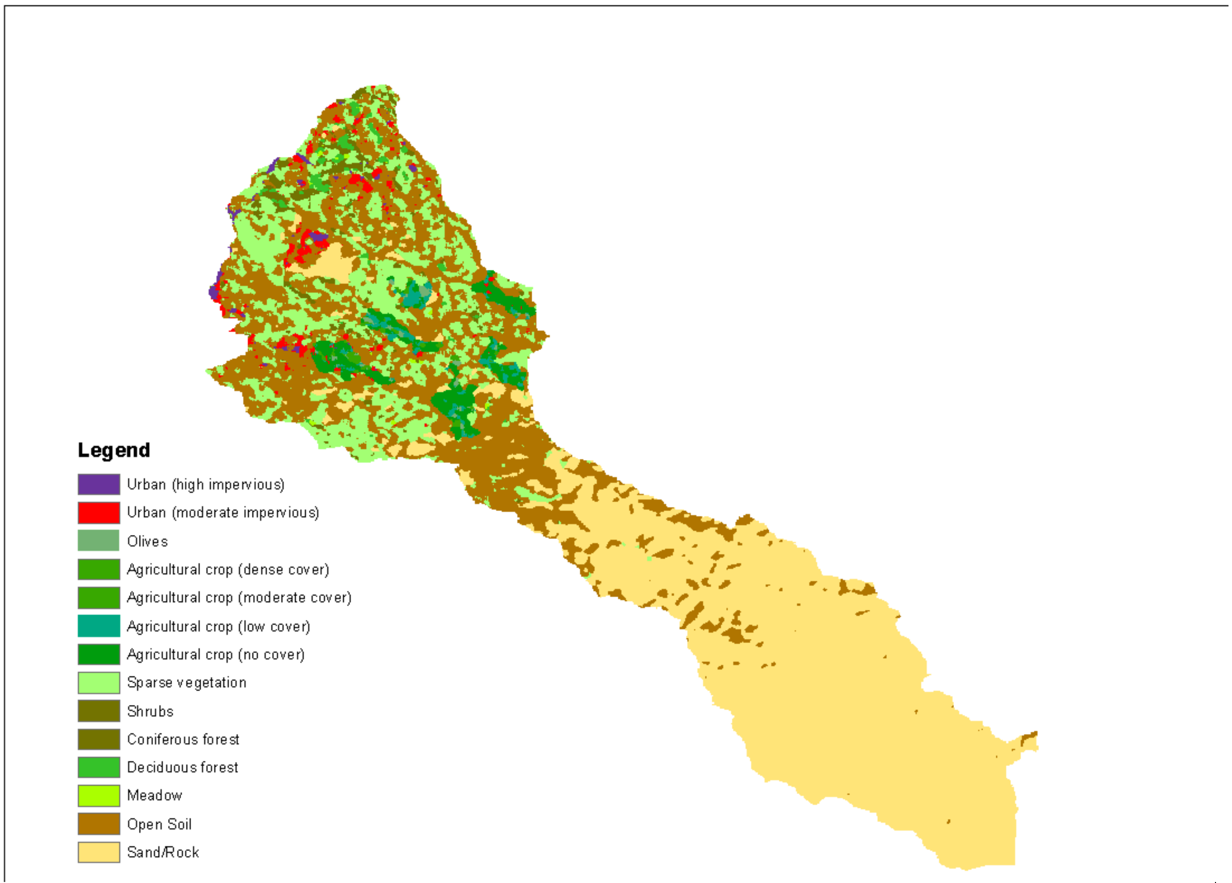

Figure3.5. Land covers of Darga catchment.

4. DESCRIPTION OF THE MODEL

4.1 Model's structure

J2000g is a conceptual, spatially distributed, hydrological model. The model is a simplified version of the more complete J2000 model (figure 4.1). It simplifies many of the complex hydrological relationships within J2000 and has a reduced number of parameters to be calibrate. It can calculate temporally aggregated, spatially allocated hydrological target sizes, and works with different discretization strategies, such as response unit, grid cells, and catchment areas. J2000g (figure 4.2) uses a modelling environment called JAMS, Jena Adaptable Modeling System, which is a JAVA-based modeling framework system for the development and application of environmental models. JAMS can be run independently from the operating system in a Java Runtime Environment. (Knoche et al., 2010); it was developed to accomplish three main characteristic (Krause and Kralisch, 2005):

- All process implementation need to be technically independent from the spatial representation of the simulated catchment,
- Spatial and temporal domains can be arbitrary configured by the users,
- The system must be able to integrate process from simple empirical to complex physically based algorithms.

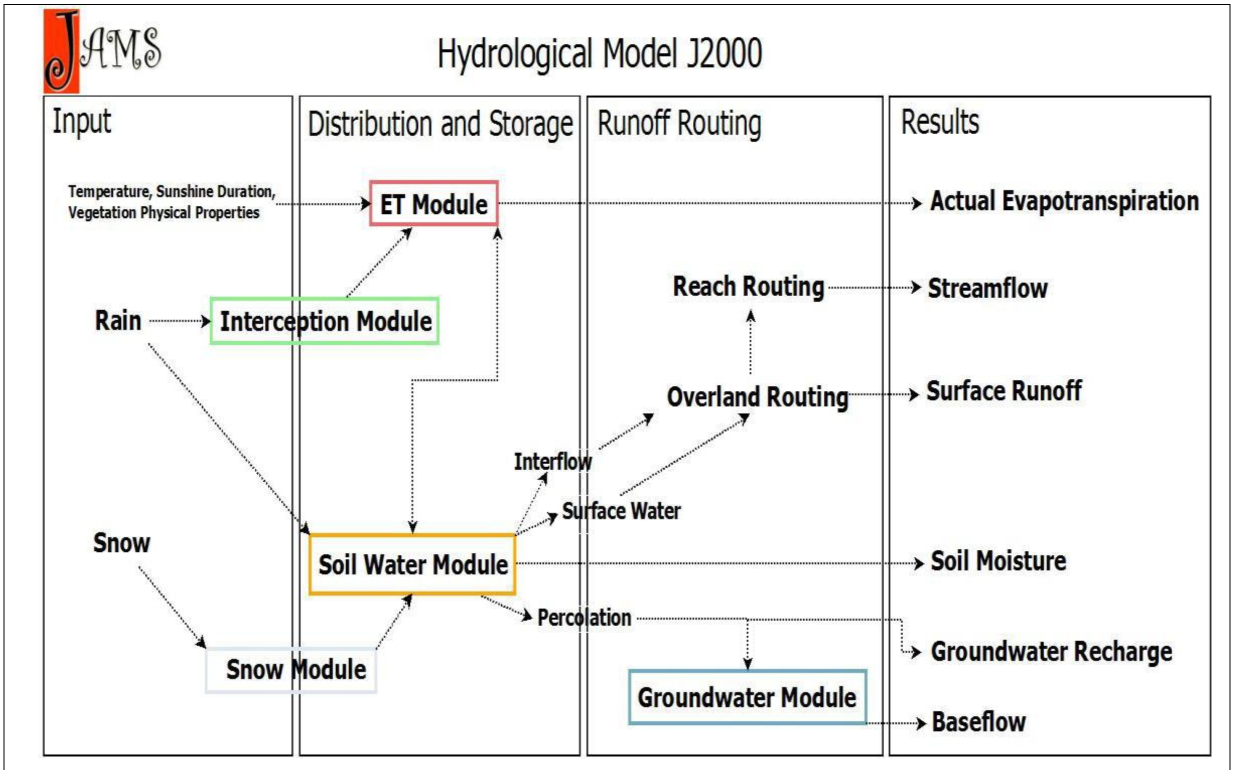

Figure 4.1 Structure of the hydrological model J2000. (Knoche et al., 2010)

The model needs spatially distributed information regarding topography, soil, hydro-geology and land use; each information has to be available for every model unit in the catchment, where model units are the areas in which the catchment is divided with the assumption that characteristics in each area can be considered having homogeneity. Then the model needs meteorological input data which have to be in the same time frame in which we want the output to be; the information required is about temperature, humidity, precipitation, wind speed, hours of sun and runoff.

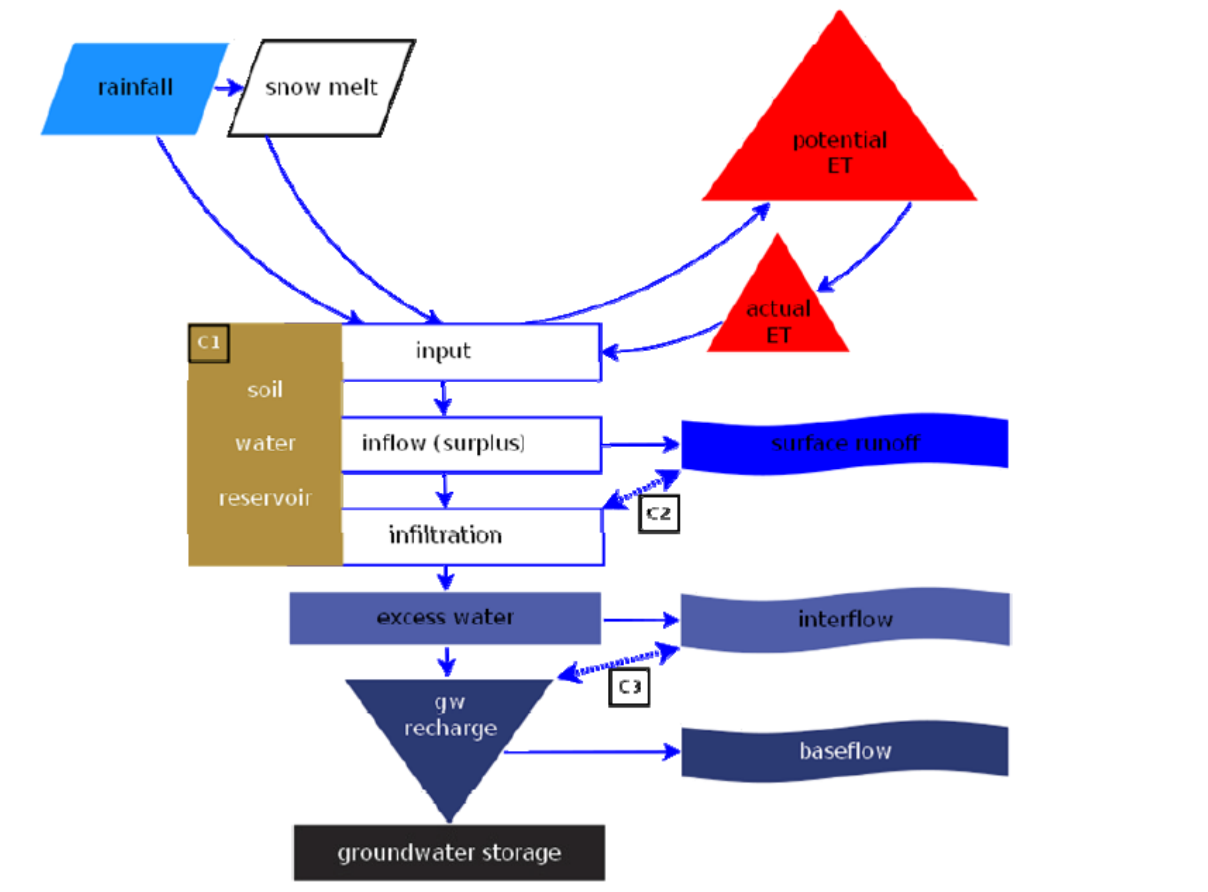

Figure 4.2 Structure of the hydrological model J2000g. (Knoche et al., 2010)

To model Darga catchment we used hydrological response unit and daily time step with a simulation period of 10 years, from 03/01/2003 to 25/12/2012. Hydrological Response Unit (HRU) are homogenous entities delineated by GIS analysis of relevant spatially distributed information (Rödiger et al., 2008), every HRU has unique value of area, elevation, slope, aspect, land-cover and soil type (figure 4.3). For each HRU and each time step climate input are calculate using an inverse-distance-weighting interpolation with optional elevation correction. The process of regionalization has the purpose to switch from punctual values (the measured values available in some stations) to spatially distributed values, one for each model unit (HRU). The steps are the following (from ILMS-Wiki, 2011):

1) Calculation of a linear regression between the station values and the station heights for each time step. Thereby, the Squared Correlation Coefficient (R^2) and the slope of the regression line (bH) is calculated.

2) Definition of the n gaging stations which are nearest to the particular model unit. The number n which needs to be given during the parameterization is dependent on the density of the station net as well as on the position of the individual stations.
3) Via an Inverse-Distance-Weighted Method (IDW) the weightings of the n stations are defined dependently on their distances for each model unit. Via the IDW-method the horizontal variability of the station data is taken into account according to its spatial position.
4) Calculation of the data value for each model unit with the weightings from point 3 and an optional elevation correction for the consideration of the vertical variability. (The elevation correction is only carried out when the coefficient of determination – calculated under point 1 – goes beyond the threshold of 0.7.)

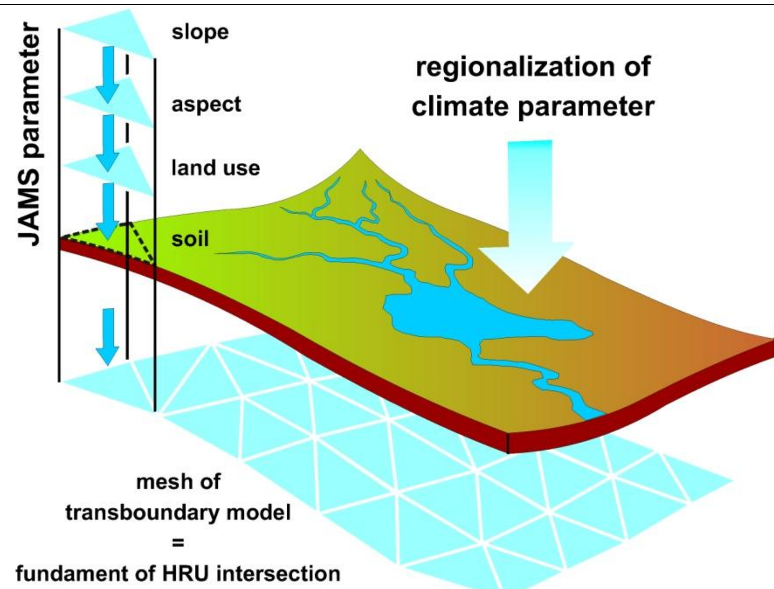

Figure 4.3 The concept of HRU derivation.

The calculation of the data value for each model unit (DW_U) without elevation correction is carried out with the weightings (W(i)) and the values (MW(i)) of each n gaging station according to:

$$DW_U = \sum_{i=1}^{n} MW(i) \cdot W(i)$$

Correction reduces the systematic errors which generally occur in the measurement. For the calculation with elevation correction the elevation difference (HD(i)) between the gauging station and the model unit as well as the slope of the regression line (b_H) are taken into account. Thus, the data value for the model unit (DW_U) is calculated according to:

$$DW_U = \sum_{i=1}^{n} ((HD(i) \cdot b_H + MW(i)) \cdot W(i))$$

The geographic coordinate system used for the input data was WGS 1984, The World Geodetic System dating from 1984, and the Projected Coordinate System was WGS 1984 – UTM Zone 36N, the Universal Transverse Mercator coordinate system suitable for the area of Israel.

4.2 Model output

The output of the model consist of: runoff, potential and actual evapotranspiration, actual and relative soil moisture, groundwater recharge. The model run autonomously in each model unit and calculates the outputs, then runoff concentration and retention are calculated as summation of the model units to the direct runoff, lateral flow and base flow utilizing the Nash cascade method.

4.2.1 Evapotranspiration

The J2000g model calculates the potential evapotranspiration (PET) using Penman-Monteith equation (Krause and Hanisch 2009; Krause 2002) which is said to be the best adapted evaporation approach due to its physical background (Dunger, 2004). Actual evapotranspiration (AET) is regarded as the amount of water that evaporates under the constraint of the actual water content of soils; it is calculated as function of potential evapotranspiration and soil moisture by reducing the PET values in relation to the soil moisture budget according to the following function:

$$aET = \left(\frac{actMPS}{LinETRed * maxMPS}\right) * pET$$

Where actMPS is actual saturation of MPS (i.e. mid pore storage); maxMPS is the maximal saturation of MPS and LinETRed is a calibration parameters ("linear ET reduction coefficient"). The maximum saturation of MPS is the volume of the field capacity.

4.2.1.1 Penman-Monteith equation

Evapotranspiration is a component that can be really significant in the study of the water balance. Usually it is not emphasized as it should because it's hard to verify predictions with direct measurements, which are more affected by uncertainties than other components such as rain and runoff. There are lot of method to estimate evapotranspiration, in this study we have used one of the most popular, the Penman-Monteith equation. It is an equation developed by John Monteith (Monteith, 1965) to estimate the evaporation of water from a surface with vegetation. The equation was derivate by the previous equation of Howard Penman (Penman, 1948), who combined the energy balance with the mass transfer method and derived a method to calculate the evaporation from an open water surface, based on standard climatological values of sunshine, temperature, humidity and wind speed (www.fao.org). That's why in its final denomination it has the name of both the scientists. Penman's equation is the following (Terry, 2004):

$$\lambda \mathrm{E} = \frac{[\Delta(R_n - G)] + (\gamma \lambda E_a)}{\Delta + \gamma}$$

where:

- λE is the evaporative latent heat flux
- λ is the latent heat of vaporization (usually a constant value of $\lambda = 2.45$ is taken, which is the values at the temperature of 20ºC)
- Δ is the slope of the saturated vapor pressure curve

- R_n is net radiation flux
- γ is the psychrometric constant (0,066)
- Ea is the vapor transport flux
- G is the soil heat flux.

From this equation the Penman-Monteith equation was derived, It takes in account particular vegetation parameters such as stomata resistance and leaf area index and include also a bulk surface resistance term. The equation is nowadays used for evapotranspiration calculation by The Food and Agriculture Organization of United Nations (FAO) and The American Society of Civil Engineers, among others. Its formulation, for daily values, is the following (Terry, 2004):

$$\lambda \mathrm{ET_o} = \frac{[\Delta(R_n - G)] + \frac{86400\,\rho_a C_P (e_s^o - e_a)}{r_{av}}}{\Delta + \gamma\left(1 + \frac{r_s}{r_{av}}\right)}$$

where the new terms represent:

- ρ_a is air density,
- C_P is specific heat of dry air,
- e_s^o is mean saturated vapor pressure calculated as the mean e^o at the daily minimum and maximum air temperature,
- r_{av} is the bulk surface aerodynamic resistance for water vapor,
- e_a is the mean daily ambient vapor pressure,
- r_s is the canopy surface resistance

The equation take in account parameters that influence, from uniform zone of vegetation, energy exchange and corresponding latent heat flux (evapotranspiration). Most of this values come from measurements or can be calculated from weather data. The result of this equation can also be expressed as the evapotranspiration of a big leaf described by two groups of parameters, one characterized by atmospheric physics and canopy architecture (r_{av}, r_s) and the other one by the biology of the surface (light attenuation, leaf stomatal resistances, etc.) and environmental conditions (irradiance, vapor pressure deficit, etc.).

Bulk surface aerodynamic resistance control the flux of heat and water from the evaporating surface to the air above the canopy according to this equation (Terry, 2004):

$$r_{av} = \frac{\ln\left[\frac{z_w - d}{z_{om}}\right] \ln\left[\frac{z_r - d}{z_{ov}}\right]}{k^2 U_z}$$

Where:

- z_w height of wind measurements
- z_r is height of humidity measurements,
- d is zero plane displacement height,
- z_{om} is roughness length governing momentum transfer,
- z_{ov} is roughness length governing transfer of heat and vapour,
- K is the von Karman's constant (0.41),
- U_z is wind speed at height z_w.

The equation is written for climatic conditions near the adiabatic ones, which means no heat exchange or a really small one, and for long time steps. The use of the equation for short time periods needs the addition of corrections for stability.

Canopy surface resistance describes vapour's flow resistance through the transpiring surface. Where the soil is not completely covered by vegetation, there is an effect of evaporation from soil surface. Canopy surface resistance is also influenced by the water content of the vegetation. The following formula is an approximation of the real behavior of that parameter (www.fao.org):

$$r_s = \frac{r_l}{LAI}$$

Where:

- r_l is stomatal resistance of the well-illuminated leaf,
- LAI is leaf area index.

4.2.2 Soil water budget

The soil water budged is the component of J2000g that distributes the water present in the system, coming from rain and eventually snow, in the different output storage. Water is first send in the evaporation module until the value of potential evapotranspiration is reached. After that the surplus is divided, by some parameters of the model, between runoff and infiltration. Infiltration goes in the soil water storage and from there the excess of water is divided between lateral flow and groundwater recharge. This partition is controlled by slope and a parameter calibrate by the user.

4.2.3 Snow cover

Model can also calculate snow cover in function of two values of temperature:

- accumulation temperature, mean between T_{min} and $T_{average}$
- Melting temperature, mean between $T_{average}$ and T_{max}

Based on these values a snow melt factor is calculated. In this study snow module was totally ignored because the occurrence of snow in the area can be disregarded.

4.3 Model's parameters

Parameters of the model have to be configured by the user to make the model prediction fit with observed values in the phase of calibration. All the J2000g parameters are listed and described below, with brief discussion of their control on main hydrological process.

InitSoilWater.FCAdaptation: It is the adaption factor which multiplies the absolute pore volume of the soil and defines the water volume which can be stored in the soil component of the model. It controls soil moisture; if the value is high groundwater recharge decreases because less water goes in the ground; actET increase because more water is stored in the soil and can evaporate.

SoilWater.lat.VertDist: it controls if water goes to groundwater recharge or to interflow, if the value is small most of the water goes to the groundwater recharge, if it is higher more water goes to the lateral runoff.

SoilWater.linETRed: Actual ET is calculated as a function of PET and actual soil moisture. The linETred parameter is a reduction coefficient, which directly decreases AET and therefore increases actual soil moisture. With increasing soil moisture in the model more water is available for all runoff components, including direct runoff (RD1), lateral runoff (RD2) and also percolation (=GWR). As a result, groundwater recharge can partly be increased, by reducing the AET by choosing a larger linEtred factor.

SoilWater.petMult: when this value increases actET also increases and runoff decreases because less water flows in the basin; PetMult increases or decreases the absolute potential evapotranspiration and is therefore an energy balance parameter. Increasing PET values also leads to increasing AET values and therefore to decreasing soil moisture storage in the model. When less water goes in the soil water storage, all runoff components are affected and have smaller values.

SoilWater.maxPercAdaptation: it controls the maximum percolation (means maximum recharge) per day in mm. When decreasing this value, groundwater recharge is limited and direct and lateral runoff increase. The parameter doesn't affect actET.

Alpha (α): it is the distribution coefficient for the two groundwater components and controls the heavy that the model gives to the fast and slow component of the groundwater; in fact, the model simulates the recharge of an aquifer having double porosity. Low alpha values mean that the prevalent component of the groundwater recharge is the slow one, high values mean that the fast component is the most important one. In this area the dynamic of the recharge is better described by the fast component, so α=0.7 is chosen, which means 70% fast component and 30% slow one.

k1 and k2 are recession parameters to slow down baseflow.

n1 and n2 are the numbers of storages for each groundwater cascade.

5. INPUT DATA

5.1 Meteorological input data

The model needs spatially distributed information about temperature, humidity, precipitation, wind speed and hours of sun, for all the stations available around and in the study area, in order to make the most precise interpolation as possible and obtain spatially distributed inputs for the area. Every station has to be labeled with a name and a unique identification number, and characterized by coordinates and the value of elevation. Series in every station have to be complete for all the period of the model simulation and for all missing values must be coded as -9999.

Meteorological data come from different sources, mostly local authorities such as Israeli Meteorological Service (IMS) and Palestine Meteorological Service (PMS) and, were not enough, satellite data.

As said before not all the time series of every station has to be complete of real values, there can be some missing values (-9999), but it is necessary that for every time step (in our case for every day) there is at least one value available; if not, the interpolation is not possible and the model cannot run in that day (running fails and an error message is shown). If there is only one value available for a day, interpolation is not needed and this value is taken as the one for all the catchment.

The model requires maximum minimum and average daily temperature values, there are values for 26 stations around and in the catchment; the measure unit is Celsius degree. Daily average temperature is showed in figure 5.1; it ranges from 5 to 35 degree.

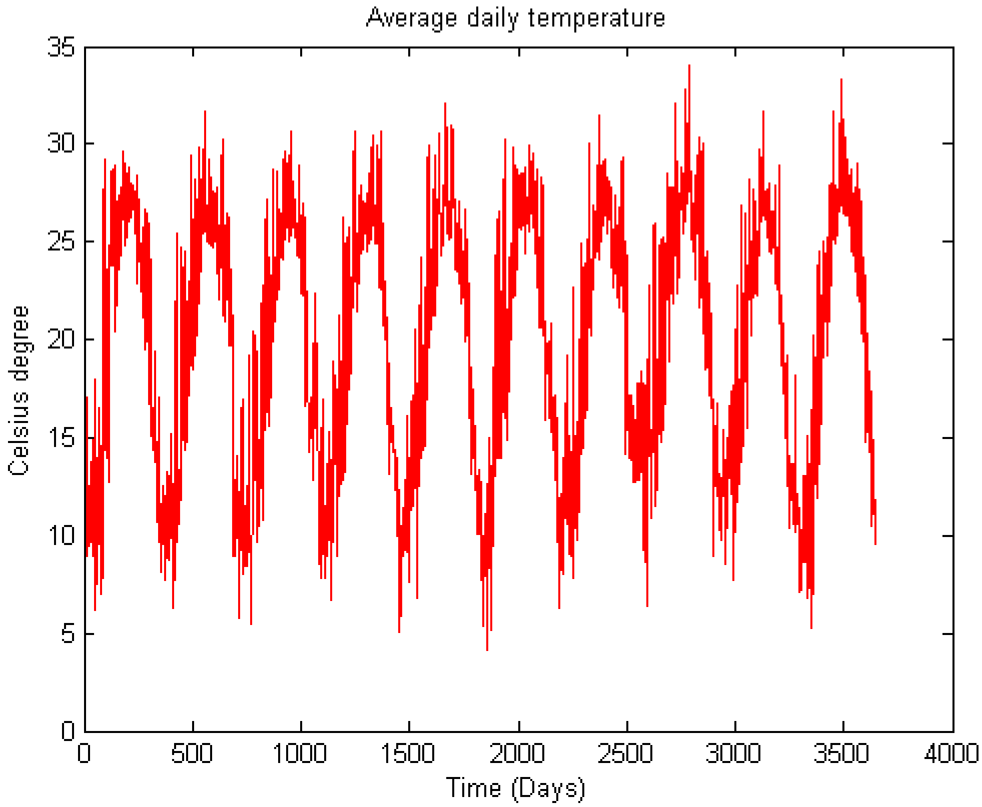

Figure 5.1. Daily average temperature in Darga catchment.

Concerning humidity the values needed are relative and absolute humidity. Absolute humidity is the water content of air, indicates the amount of water vapor (g) per unit volume (cm^3); its measure unit is g/ cm^3. Relative humidity is express as percent, so it has no measure unit, it range from 0 to 100. For Absolute humidity there are 8 stations with available values, for Relative humidity 13 stations.

Precipitation is one of the most important input variables needed by the model for performing hydrological prediction; we had access to time series collected at 28 stations. For this input we make a further restriction in the chosen of data, to be sure about the quality of the interpolation: for every day the stations with available values are enough to cover an area equal or bigger than the catchment, which means connecting all the stations with values for each day we obtain an area that entirely includes the catchment. In this way we are sure that the distributed input coming from the interpolation is in every time step a good description of the reality because it is generated by an appropriate number of stations, in fact, for every day there are at least three stations available with values (the smallest number of points to make an area). Measure unit is mm. before the simulation punctual values of every station are interpolated by the model in order to provide a distributed trend of the precipitation in the area (figure 5.2)

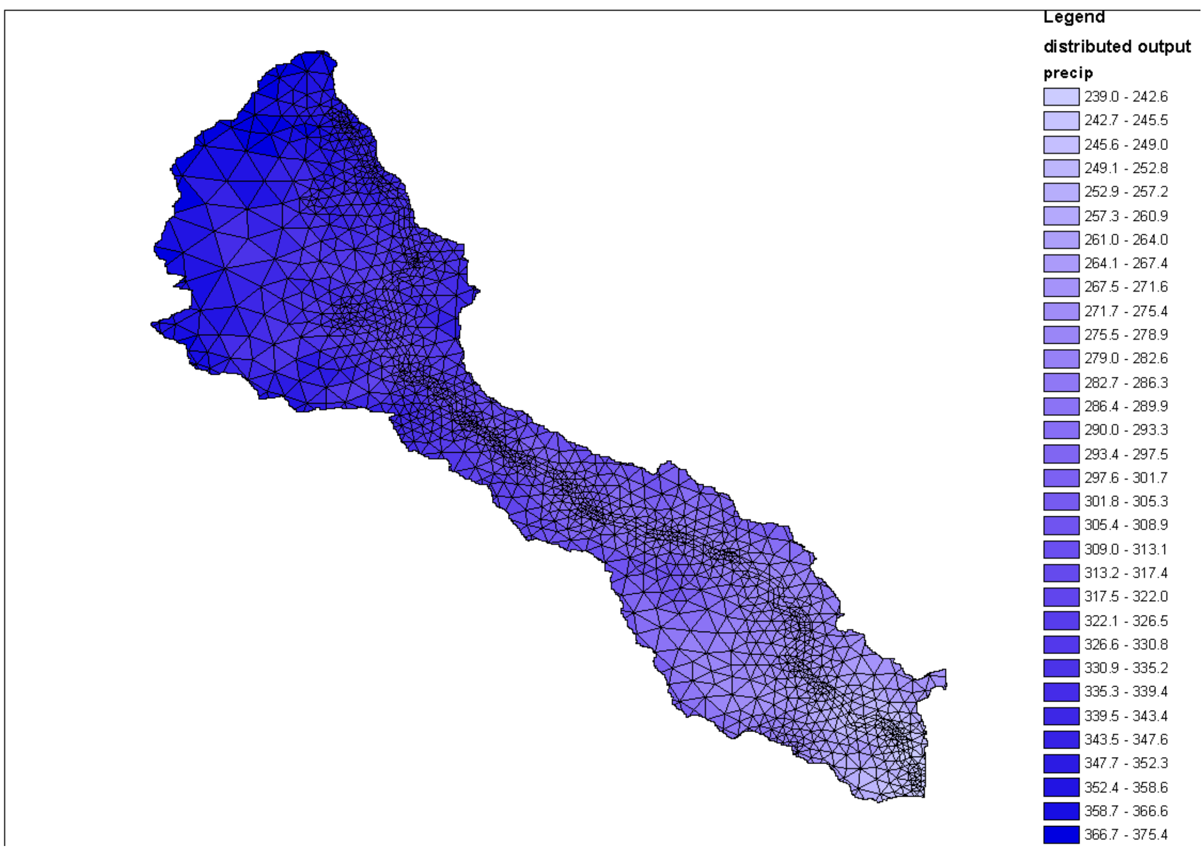

Figure 5.2. Distributed precipitation coming from the interpolation of measured values from 28 stations surrounding and within the study catchment, the map shows the rainfall depth assigned to each one of the triangular HRU.

Wind speed input requires the daily speed of the wind in m/s, the stations with available time series are 13.

Concerning the hours of sunshine, we used a mix of measured values and satellite values because we had only 2 stations with measured values and the time series were not long enough to entirely cover the run period of the model, so we downloaded a complete time series for the period 2003-2010 from ERA database to complete the missing values (http://www.era-envhealth.eu)

In addition to the meteorological input discussed above, J2000g needs a runoff series in the catchment outlet for comparison purposes; we provided this file to the model, even though all values except for 42 days were missing values.

5.2 Catchment's input data

Four tables describe the catchment regarding topography, soil, hydro-geology and land use. Each table has to start with "#name of the table" and close with "#end of file".

The most important table the model needs is called HRU_surface which contain all the information about surface and structure of the catchment (figure 5.3). The model calculates the hydrological output variables in each HRU and for each time step. HRU network in this catchment counts 3160 units and for every time-step calculations will be done for each of this units. In the table each HRU is defined by an ID number (-), the extension of the area (m^2), the coordinates of the central point of the HRU area (°, WGS84), elevation (m), slope (°) and aspect (°). Moreover the table contain other three ID (-) which refers to other three tables contain information about soil, land use and hydrogeology.

# hru.par									
ID	x	y	area	elevation	slope	aspect	soilID	landuseID	hgeoID
0	0	0	0	0	0	0	0	0	
9999	9999999	9999999	9999999999	10000	90	360	9999	9999	99
n/a	m	m	m2	m	deg	deg	n/a	n/a	n/a
45	721576.9	3502610	17632.31581	214	12.5641	180	22	20	
64	715380.6	3506168	9.932611059	412	33	11.25	3	20	
69	716954.9	3505036	106.1452189	337	21	90	22	20	
88	713576.1	3510474	166.7238471	551	4	90	15	15	
100	721631.8	3502141	89.43776891	224	28	90	22	20	
115	723040.1	3499926	5057.522796	49	22.47059	135	26	20	
125	715199.9	3506356	96.96602429	435	25.5	135	3	19	
129	715432.2	3506096	3425.202917	450	23.23077	45	3	19	
133	716909.5	3505429	166.328495	339	6.5	180	22	20	

Figure 5.3. HRU table

Following there are the three more table needed:

Hgeo: the table contains the IDs which refer to the ones of the HRU table and for each ID a value of the maximum possible percolation rate per time interval in mm per time unit. This value can also be seen as the maximum ground water recharge can occurs in the geology formation.

Landuse: contains vegetation parameters that are needed for evapotranspiration calculation according to Penman-Monteith equation. For the ID of each land use unit have to correspond:

- a description of the land use (urban, olive, agricultural crop, etc.);
- value of albedo (-);
- values of stomata resistances for good water availability (s/m) for the months January to December;
- values of leaf area index (m^2/m^2) for four Julian days (110, 150, 250, 280) for a terrain height of 400 m above the sea level;
- values of effective vegetation height (m) for the same Julian days as before (110, 150, 250, 280) for a terrain height of 400 m above the sea level;
- value of effective root depth (dm);
- Value of sealed degree (%).

Albedo is defined as the ratio of reflected radiation from the surface to incident radiation upon it. Being a dimensionless fraction, it is expressed as a percentage, in a scale from 0 to 1, where 0 means no reflecting power of a perfectly black surface, and 1 means a white surface with perfect reflection power.

Stomata Resistance is the opposition of the stomata of a leaf to the passage of carbon dioxide (CO_2) entering, or water vapor exiting through it. Stomata are small pores on the top and bottom of a leaf that are responsible for taking in and expelling CO_2 and moisture from and to the outside air.

Leaf area index is a variable dimensionless defined as the total one-sided area of green leaves in a vegetation canopy relative to a unit ground area. LAI ignore canopy details such as leaf angle distribution, canopy height or shape.

Julian day refers to a continuous count of days from 1 January to 31 December; an integer is assigned to each whole solar day. The four days required by the model are:

- 110 → 20 April
- 150 → 29 May
- 250 → 6 September
- 280 → 7 October

Sealed degree is a percent number, in a scale from 0 to 1, describing how much the water infiltration is allowed. For example, a road with asphalt doesn't allow any infiltration so the degree of sealing should be zero.

Soil: the table contains soil-physical parameters for each soil unit that occurs in the catchment:

- SID, integer that represent an unique ID that connects this table to the HRU table
- Depth, Depth of the soil (cm)
- Fc_sum, Entire usable field capacity of the soil (mm)
- Fc_1 to fc_n, usable field capacity for each decimeter in mm/dm

Field capacity is a hydrological constant of each soil, definable as the amount of soil moisture or water content held in the soil after excess water has drained away.

6. GIS-BASED HYDROLOGICAL ANALYSIS

The aim of this chapter is to describe in a detailed way all the steps to derivate the shape of the catchment and to extract all the useful information from the area that we can obtain making an hydrological analysis with a GIS system. The starting point is the previous knowledge of the digital elevation model (DEM) and the position of the basin's outlet.

6.1 Management of information in a GIS system

GIS is the acronym of Geographic Information System. GIS environments store, represent and analyze geo-referenced information, which means data whose geographic coordinate are known.

There are two type of data:

- Vector data: graphical geo-referenced objects (points, lines, poligons, etc.).
- Raster data: generally rectangular grids of cells, where each cell is characterized by coordinates and an assigned value.

Vector data can also be divided in three different categories:

- Points: a set of coordinates (x,y) defining a set of points, and each point is linked with a record of information in the database. There is an univocal connection between point and its record.
- Lines: object with the shape of segment whose vertexes are geographically known. Every feature is linked with a record in the database table (table of attributes)
- Polygons: object representing closed area, its vertexes are known and the all area can be linked with some data.

6.2 Basic definitions

Digital elevation model (DEM) is the spatially distribution of altitude in an area, in digital format. It is usually a raster file in which every point is linked with its value of absolute height. (figure 6.1)

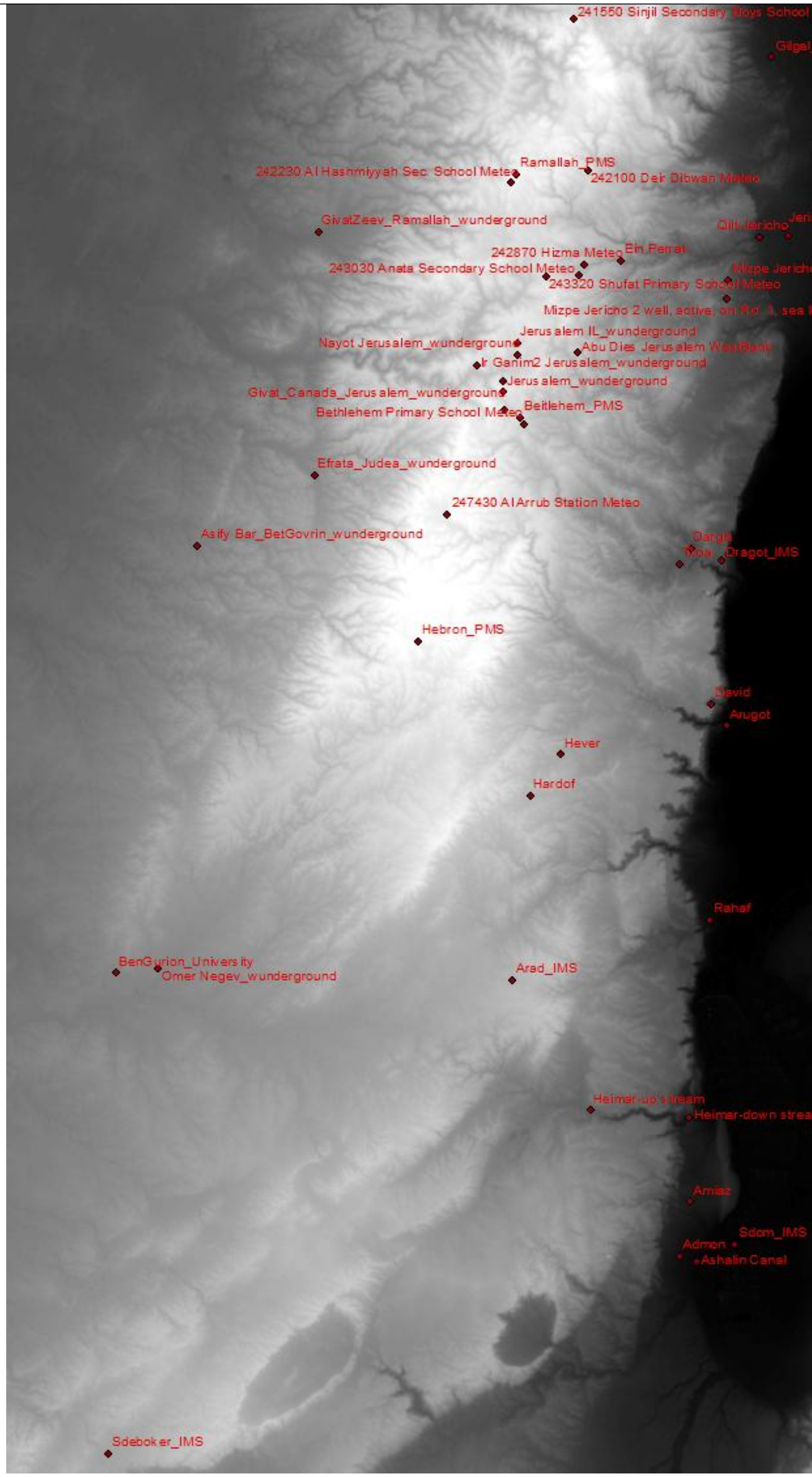

Figure 6.1 DEM and measurement stations in the study area.

In this study DEM, measurement stations' coordinates and all the other data loaded in GIS are referenced in the UTM system. The Universal Transverse of Mecator is a projection of the terrestrial surface on a plane, it describes all the world's surface but North and South poles, in which another projection is used. In UTM system Hearth is divided in 60 time zones, each one 6° longitude large. Moreover it is divided by parallels in 20 "belts" of 8° latitude. The intersection of time zones and "belts" generates zones, every point on the terrestrial surface belong to a zone and is described by unique values of latitude and longitude.

For derivation of the catchment's shape and the others hydrological characteristics of the study area, we will use the "*Hydrologytools*" of ArcGis.

6.3 Derivation of Darga catchment's shape

Calculation of the "Flow Direction": this function creates a raster with the flow direction of every cell to the downstream one according to the "highest slope" criterion. This means the function simulate the natural direction of fluid's particle from one cell to the next (figure 6.2). We have to put the DEM file as input.

A perfect "Flow Direction" should contain only 8 values, which represent the 8 cells neighboring in which the water can flow because we are working in a simplified reality where space is divided in square cells. But the first Flow Direction calculated has more than just 8 values, we can observe that looking in the Attribute Table of our file. Some of this values represents sinks, cells in which water can't flow nowhere because all the neighboring cells have higher altitude. Sinks are depression into the DEM which can represent real topography's depressions or errors in the data. There a function in ArcGis to identify sinks and correct them if they belong to the second group. We used "Sink" function (*ArcToolbox>Spatial Analyst Tools>Hydrology>Sink*): we put Flow Direction raster file as input and obtain the map of sinks in the area (figure 6.3).

	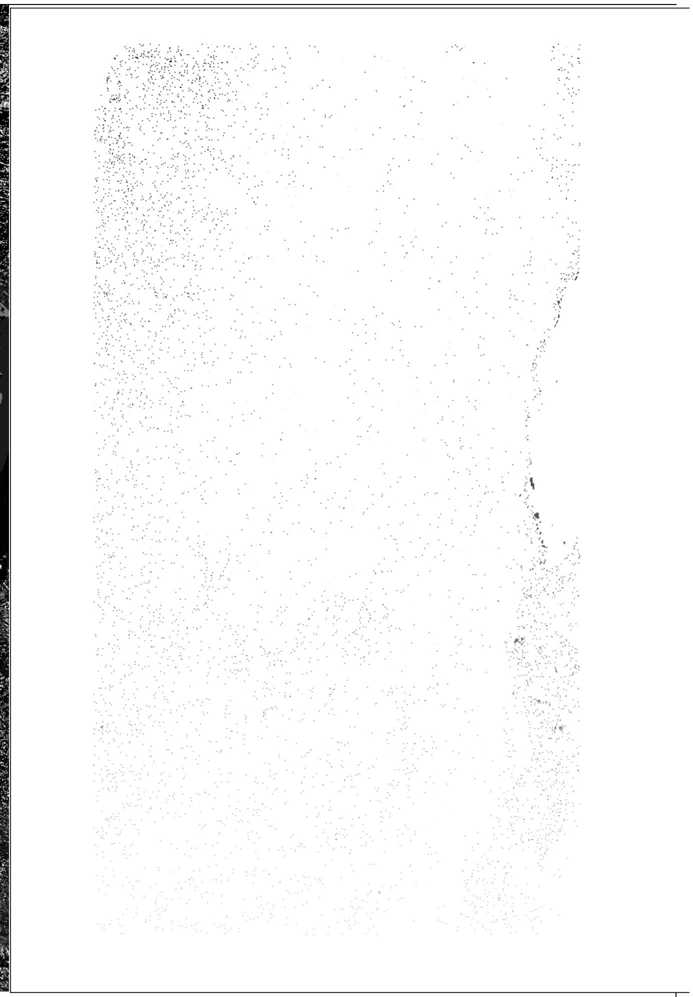
Figura 6.2 Flow direction.	*Figure 6.3 Sinks.*

The output is a set of black points which represents depressions (figure 6.3) into the DEM. In our case this depressions interrupt somewhere the principal river of the catchment, this is completely in contrast with the definition on catchment because the water cannot flow to the outlet point. So this case depressions have to be filled with the "Fill" function: correction consists in increasing the value of altitude of every sink until it has reached the minimum value of the neighboring cells. The result is a DEM with regular trend. For all the next operations the filled DEM will be used.

First, we need to recalculate a new Flow Direction, utilizing the new DEM. The procedure is exactly the same (already explained above) but the new raster file will contain only the 8 value (figure 6.4): 1, 2, 4, 8, 16, 32, 64 and 128, as explained before.

Calculation of *"Flow Accumulation"*: this function give as output a raster file containing the flux accumulated in every cell counting for each cell the total number of cells drained by that cell.

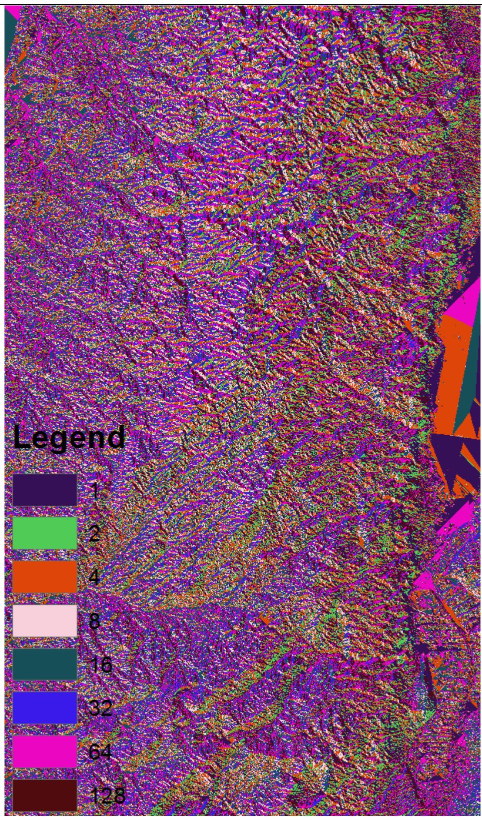

Figure 6.4 Flow direction with filled DEM.

Flow Accumulation represents the content of water that can flow in every cell, according to this assumptions:

- All the water became surface flow,
- There is no interception, evapotranspiration and loss in soil;

Flow Accumulation can be seen as quantity of rain falling in the area distributed in every cell. Cells with high value of Flow Accumulation are zones of high concentration of water that can belong to rivers, otherwise cells with value of zero are zone of high altitude and can belong to watershed.

To identify which pixels belong to rivers we used *"RasterCalculator"*: firstly we have to define a threshold: a minimum number of cells drained by one cell which characterizes that cell as belong to a river. After that we use the following syntax to give the command:

streamnetwork=Con("FlowAcc">2000,1)

where parts highlighted with yellow depend on previous operations:

- "*FlowAcc*" is the name of the raster file Flow Accumulation, if the user gave a different name to that file, in the syntax above it has to be changed in order to have the same of the raster file.
- 2000 is the value of the threshold, as said before it can change, depending on the quantity of water falling in the area

With RasterCalculator we identify pixel which belong to a river, to merge this information with the information regarding flow direction we use *"StreamLink"*. We have to put to input in this function, the one coming from RasterCalculator and the Flow Direction. Be sure the Flow Direction you use is the one calculated using filled DEM.

Once we have obtained the stream network every channel should be characterized by a number which define is order. The order of a river give an idea of how big it is, which means how many rivers flow into it. We used the function *"Stream Order"*, it takes in input the output of *"RasterCalculator"* and the Flow Direction. There are two different methods to calculate stream order:

- METHOD STRAHLER: a stream reach may increase downstream a junction, in particular the order increases in the downstream direction after junctions of two streams with the same order, otherwise the stream reach maintains the higher order of the pair (for example if two stream reaches with order 3 join together, the stream resulting from the union will have order 4; if a 2-order stream run into a 3-order stream, the downstream reach will still be a 3-order stream).
- METHOD SHREVE: takes in account every single intersection and the resulting order is simply the sum of the orders of the streams that merge into one (for example two stream, of order 2 and 3 respectively, merge into one which will have order 5).

The first method is generally more used than the second one, and it was the chosen method for this study (figure 6.6).

The next step is the creation of a shape file with the stream network. We utilized the function *“Stream to Feature”* which takes in input RasterCalculator and Flow Direction. Moreover is possible to choose an option called *“Simplifypolylines”* that corrects the angular form of the streams and make them more plausible (figure 6.7)

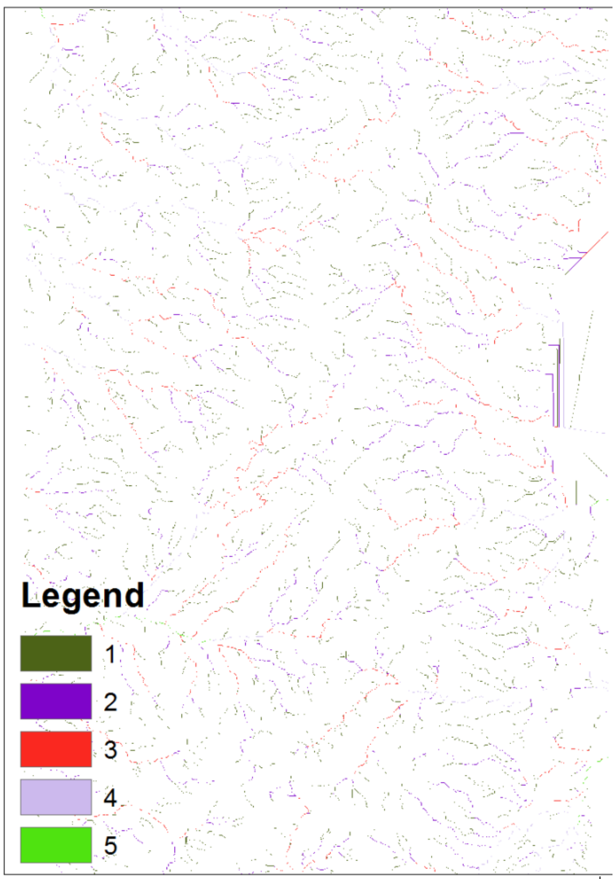

Figure 6.6 Output stream order(STRAHLER METHOD).

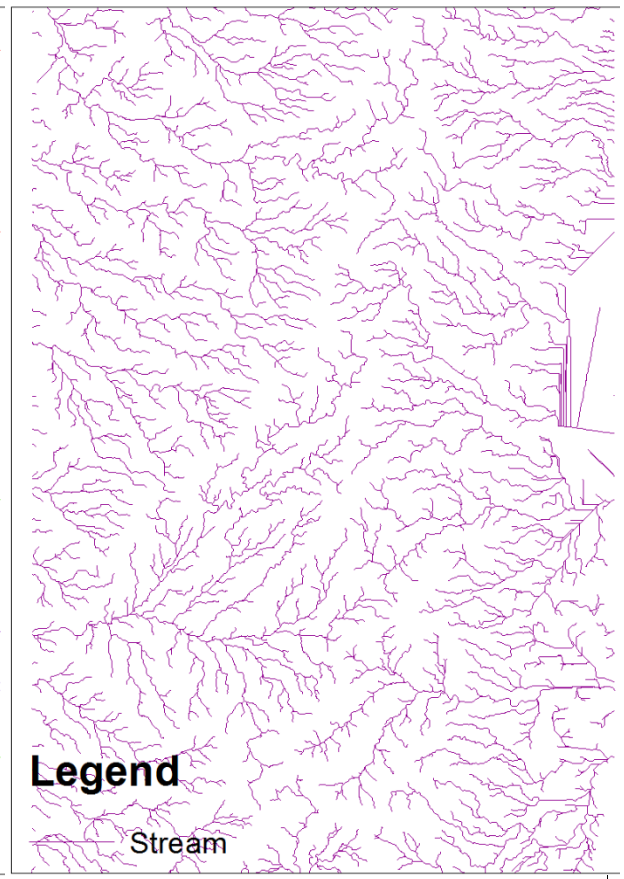

Figure 6.7 stream network.

To define basins in the area, we used the function *“Basin*, which take as input the Flow Direction and give as output raster with the basins, as shown in figure 6.8.

The next step should be to use the function *"Watershed"* to calculate the watershed of the basin in precise points correspondent to the position of our measurement stations. But utilize that function directly on the shapefile with the stations is not recommended because due to problems of projection, usually the positions of the stations don't perfectly correspond to the cells with highest water accumulation (streams). That means, in ArcGis environment, the station is not situated on the river. To avoid this problem we used the function *"Snap Pour Point"* which move stations that are not on streams to the nearest high-water-accumulation cell. Function requires to set a parameter called "Snapdistance" that approximately define the maximum distance can exist between a station and its correspondent water stream, this depends on the precision of our data. In this case the value 300 was used.
Moreover it's mandatory in this case to set the option "Union of input" to be sure that new points will stay exactly on the streams.
After that is finally possible to use the function "*Watershed"* and put as inputs flow direction and the shapefile with stations' positions (figure 6.9).

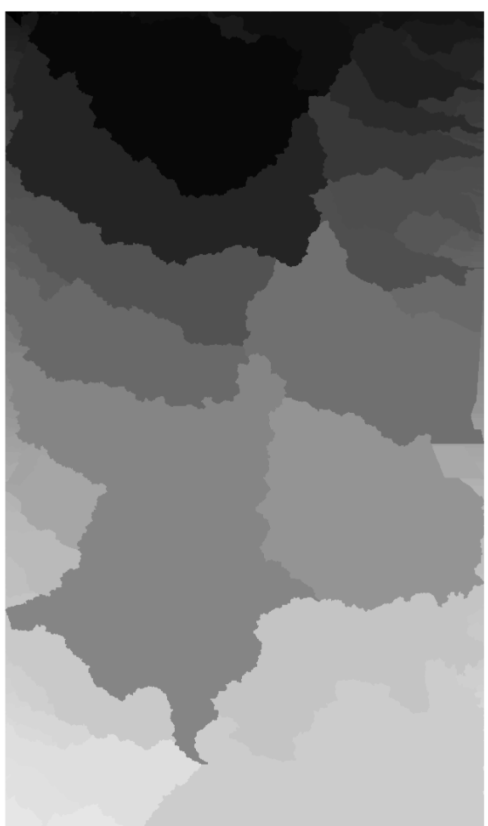

Figure 6.8 Basins.

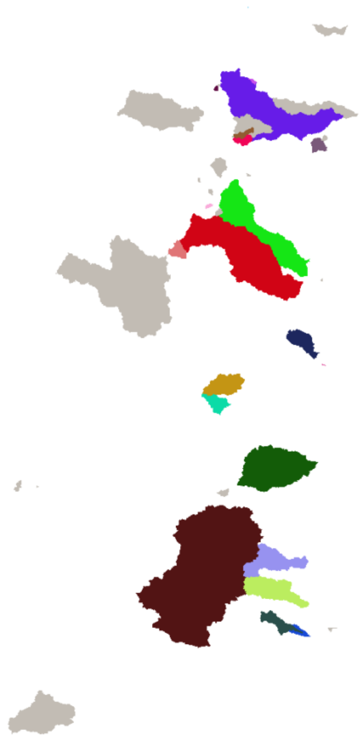

Figure 6.9 Watershed.

Every station is associated with a catchment whose outlet is the same station.

Next step is the calculation of flux's length with the function *"Flow Length"* which lead to identification of time of concentration for every catchment. The time of concentration is time needed from a fluid particle fall in the hydraulically most far point to reach the outlet of the catchment. Depends on the catchment's topographical and geological characteristics.

Calculation can be done from the top of the catchment to the outlet (Downstream) or in the opposite direction (Upstream):

- Downstream: for each cell is calculated the longest distance, through the flux's direction, to the lowest point (for example a sink) or, when it miss, to the catchment's outlet.
- Upstream: for each cell is calculated the longest distance, through the flux's direction, to the highest point of the watershed,

Function takes Flow Direction as input. Following are shown the results using both the methods (figures 6.10 and 6.11):

Figure 6.10 Flow length upstream.	*Figure 6.11 Flow length downstream.*

From this point we are finally able to extract our catchment. We utilized the function "*Raster to polygon*". We set as input the raster output of "*Watershed*" and the function will convert every catchment in a polygon (figure 6.12)

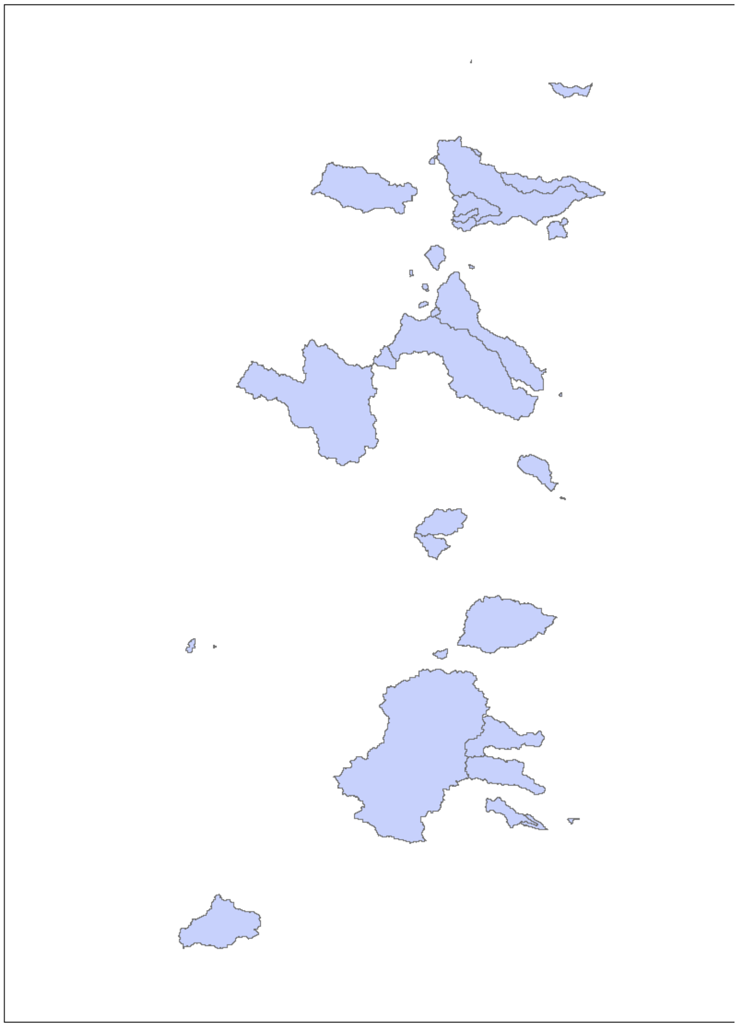

Figure 6.12 Polygons shapefile with basins associated to different stations.

To extract the catchment:

- select the catchment on the map,
- right button of the mouse on the layer window,
- choose “export”.

Using the function “Clip” we can “cut” the stream network to isolate only streams which belong to our catchment. Results is shown in figure 6.13:

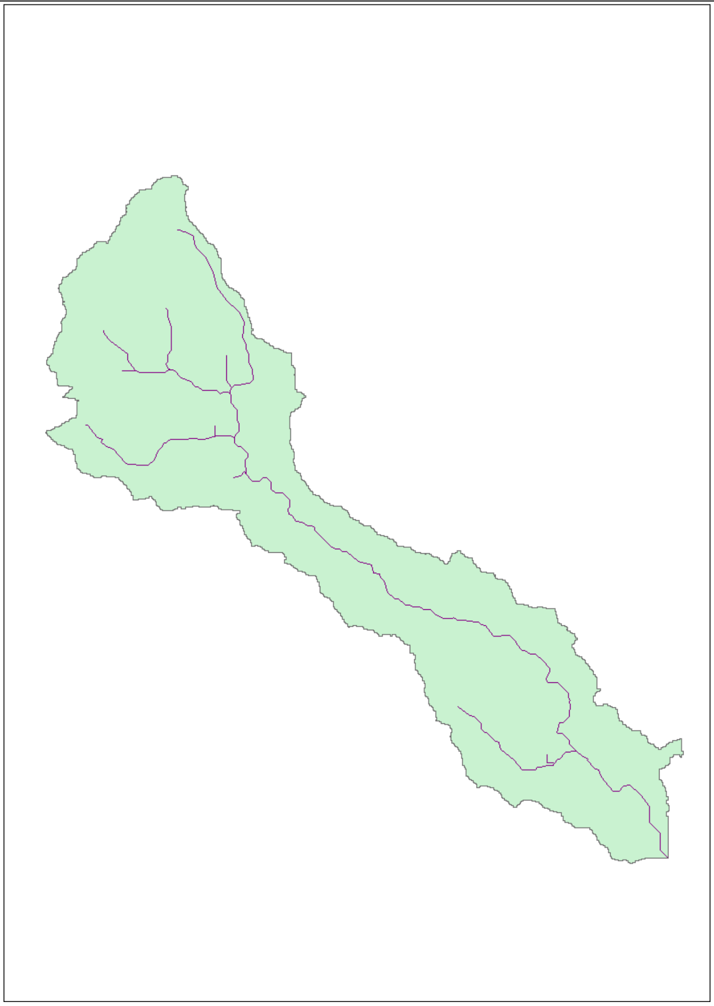

Figura 6.13 watershed of Darga catchment and his streams.

7. CALIBRATION

Because of the inadequate length of runoff data (only 42 days with observed data are available in 10 years, and most of them with an observed discharge of 0 m^3/s) a normal calibration-validation comparing simulated runoff with observed values is not possible. In this study a multi-response calibration is used and it is based on Potential evapotranspiration (PET), Actual evapotranspiration (AET), Soil Moisture and Ground Water Recharge (GWR).

The parameters of the model were changed manually in a reasonable range in order to make the model's results fitting with observed (and, where missing, literature) values. Efficiency functions such as Nash-Sutcliffe efficiency (NSE), Relative mean error (RME) and Squared Correlation Coefficient (R^2) were used to evaluate the goodness of model prediction in both the phases of calibration and validation.

Absolute and Relative Error

Absolute Error is defined as the difference between calculated value and the real one, expressed in the same unit measure of the value. It is a measure of how far is our variable from its real value.

$$absErr = X_{calc} - X_{real}$$

With:

- $absErr$: absolute error,
- X_{calc} : calculated value
- X_{real} : real value.

when is necessary to estimate the precision of a measurement usually another kind of error is used: the Relative Error, it is useful to quickly understand if the error is tolerable or not because it compare the absolute error with the real value, as showed in the following formula:

$$relErr = \frac{X_{calc} - X_{real}}{X_{real}}$$

As much relative error decrease, measurement's accuracy is higher. Usually it is expressed as a percent value, to avoid to work with decimal numbers, and with positive sign (absolute value) in order to have variability only in the range from 0% to 100%, which is easy for comparison of precisions coming from different measurements.

When there are *n* measurement, with *n* real positive number, we need to calculate the Mean Absolute Error as the sum of absolute errors of each measurement, divided by the n measurement:

$$MeanAbsErr = \frac{1}{n}\sum_{i=1}^{n}|X_{ci} - X_{ri}|$$

With:

- X_{ci} calculated value at the *i* time-step,
- X_{ri} real value at the *i* time-step.

In the same way is calculated the Mean Relative Error:

$$MeanRelErr = \frac{1}{n}\sum_{i=1}^{n}\left|\frac{X_{ci} - X_{ri}}{X_{ri}}\right|$$

Squared Correlation Coefficient (R^2)

R^2 is a measure of how the model is adapt to describe the data set we want to reproduce. It ranges between 0 and 1 and it is calculated as the square of the *correlation coefficient* which describe the linearity between covariance and standard deviations of two variables (x and y):

$$\rho_{xy} = \frac{\sigma_{xy}}{\sigma_x \times \sigma_y}$$

ρ_{xy} is the correlation coefficient

σ_{xy} is the covariance, which is a measure of how much two random variables are dependent to each other, which means how much they change together. If they show a similar trend, the covariance is positive.

σ_x and σ_y are the Standard deviations, which show how much dispersion from the mean exist in our calculated values. A high standard deviation indicates that the data points are spread out over a large range of values, otherwise a low standard deviation indicates values set very close to the mean; The standard deviation of a random variable is the square root of its variance.

the expression above, can be also explicate as following (Montanari & Castellarin, 2013):

$$R^2 = \frac{\left[\sum(x-\bar{x})(\hat{x}-\bar{\hat{x}})\right]^2}{\sum(x-\bar{x})^2\sum(\hat{x}-\bar{\hat{x}})^2}$$

Where:

x is the observed variable and $\bar{x}$ the average of all the observed values,

$\hat{x}$ is the simulated variable and $\bar{\hat{x}}$ the average of all the simulated values.

Nash-Sutcliffe efficiency (NSE)

This is one of the most used criteria for evaluation of hydrological model's response, it is dimensionless and varies in the range [-inf,1].

- For NSE<0 the model works worse than using the mean value of observed data as predictor.
- When NSE=0 the model response has exactly the same accuracy of using the observed mean, so If the model has more than one parameter it has to be discarded.
- Values of acceptable NSE are in the interval]0,1], with 1 reached only when the model output is equal to the reality (very uncommon case), so usually it is in the interval]0,1[

The equation for the calculation of Nash-Sutcliffe efficiency is the following:

$$NSE = 1 - \frac{\sum_{t=1}^{n}(x_{st} - x_{0t})^2}{\sum_{t=1}^{n}(x_{0t} - \mu_0)^2}$$

Where

- n is the total number of time-steps,
- x_{st} is the simulated value at the time-step t,
- x_{0t} is the observed value at time-step t,
- and μ_0 is the mean of the observed values.

As said before, NSE is a popular indicator of model skill but there are lot of discussions about its suitability (e.g. “Do Nash values have value?”, B. Schaefli, 2007), mostly based on the use of the observed mean as baseline, which can lead to a wrong model skill’s evaluation for highly seasonal variables basins (H.V. Gupta et al., 2009).

The parameters set found to give the better results is the one showed in figure 7.1:

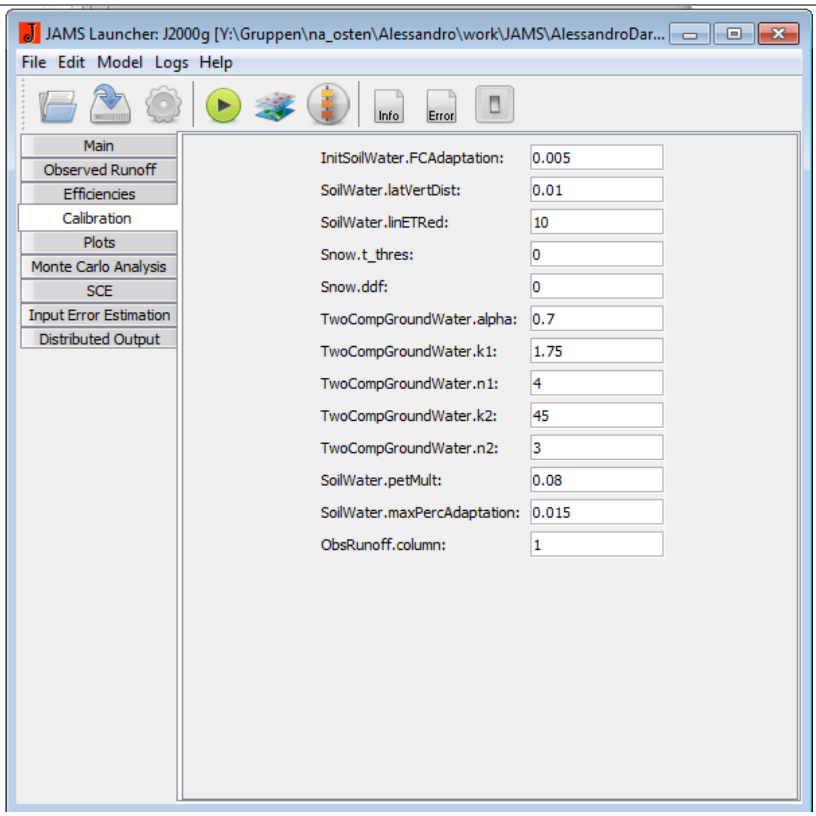

Figure 7.1. Best parameters set to fit the output model with measured values.

7.1 Evapotranspiration

Concerning potential evapotranspiration (PET), we compared the result of the model with the satellite-based Modis MOD16 dataset; these data are available for the study area only up to 2009. So the time period in which we check the goodness of the model in this prediction is the period 2003-2009. We obtained an almost perfect fit between simulated PET and satellite-based PET (figure 7.2), which means that the energy balance of the system is well described in the model. The average absolute error obtained for all of the period is 1,66 mm only.

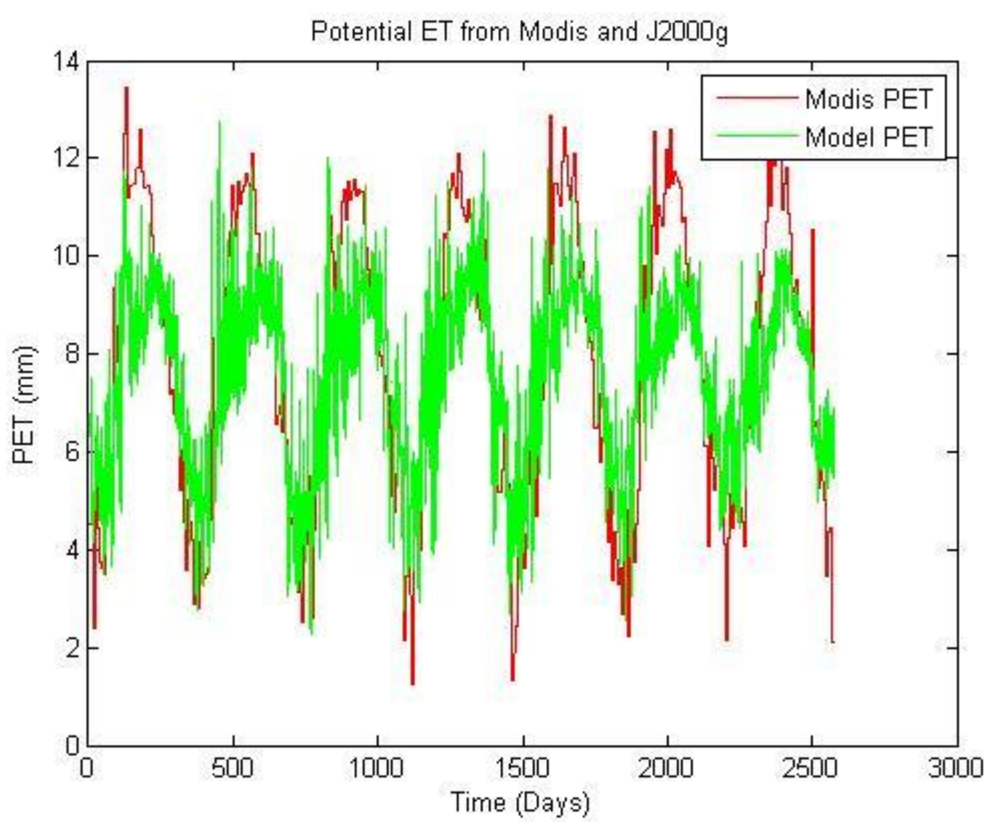

Figure 7.2. Potential evapotranspiration (PET) from Modis dataset is compared with PET simluated by the model in daily time step. The fitting is high, with an average absolute error of 1,66 mm.

Relative soil moisture calculated by the model is plotted in figure 7.3 and the trend observed makes sense because it is maximum in the winter months, and almost zero during the summer, because for the high temperature and the absence of precipitation the area is completely dry.

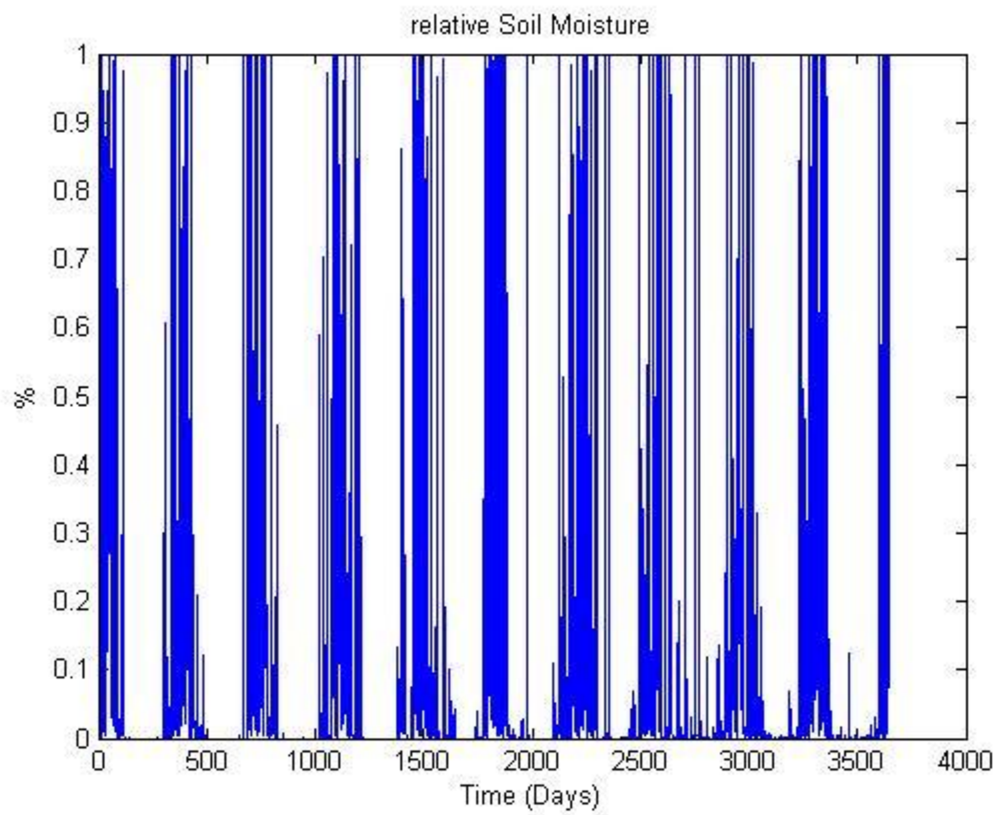

Figure 7.3. Relative Soil Moisture simulated by the model J2000g. the maximum value occurs in the winter months, during the summer the value is approximately zero because the catchment is completely dry.

Concerning AET we compare the model prediction with two satellite-based Modis data. These are Modis MOD16 and a global monthly ET estimate by Zhang et al. (2010). We used monthly values because they provide a better overview relative to daily (and also because some satellite time series are available at monthly time step only). The modeled AET and the two satellite-based estimates do not agree concerning their temporal amplitude and their range of maximum and minimum values (figure 7.4).

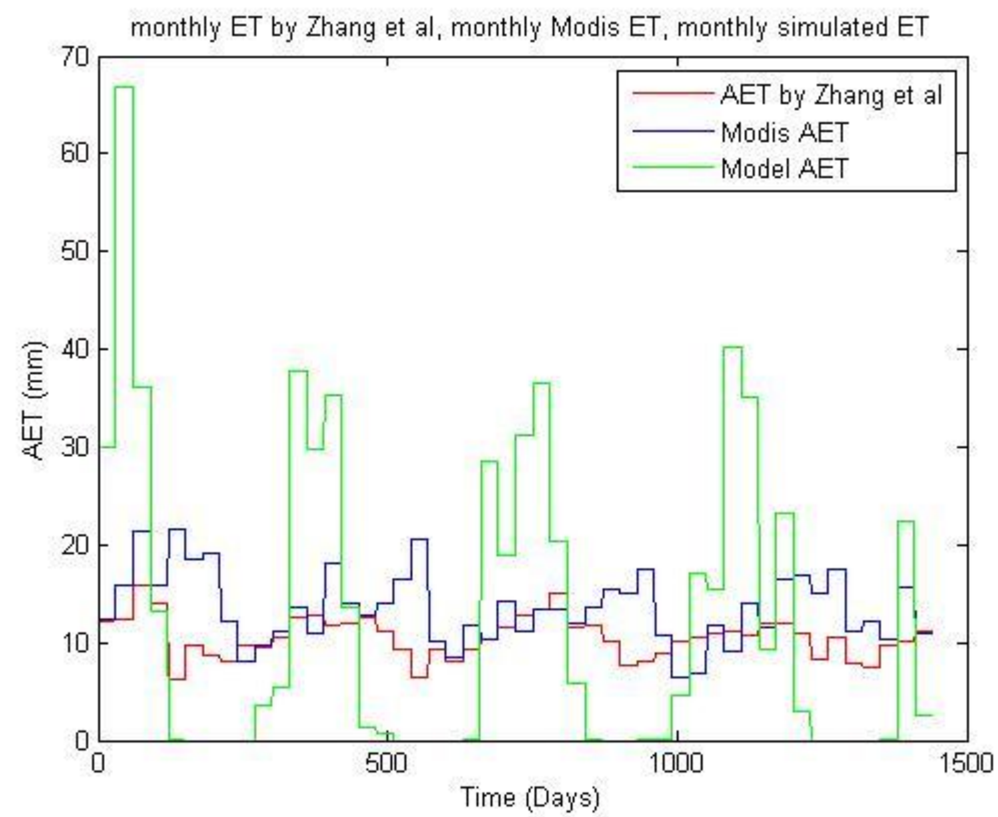

Figure 7.4. AET values simulated by J2000g give realistic values, but the curve doesn't agree with satellite data. Also the two satellite curves don't agree to each other. Is high probable that satellite values of AET in this area are not reliable.

In the model context actual evapotranspiration is a function of PET and soil moisture. As explained before, these two components have been well simulated by the model. The PET as proxy for the energy balance agrees well with the data source. The simulated relative soil moisture has realistic values, ranging from 100 percent saturation in the rain season to 0 percent in the dry season, and showing continuous amplitude. Based on a correct PET simulation and a reasonable soil moisture simulation, we assume that the AET simulation has reached a plausible range. On the contrast, both satellite-based estimates show relatively high values in the dry season, which does not make sense. Moreover the two satellite curves don't show the same trend and even not the same values. We assume, that there might be a systematic error in the satellite datasets regarding the dry season and, in general, that satellite values in this case are not completely reliable. For Modis data also another source of error was found: values are calculated only for surface with vegetation, but almost half of the study area (from the middle of the catchment right to the Dead Sea) is covered by rocks and open soil, without vegetation.

As a consequence, AET could not be calibrated directly using MOD16 satellite-based AET estimates, because the MOD16 datasets delivers unrealistic values. Therefore the simulations of actual ET were further calibrated by finding realistic values of actual and relative soil moisture. Calibrating PET and soil moisture guarantees realistic parameterization of the energy fluxes, responsible for evapotranspiration, and the available soil water, responsible for limiting the evapotranspiration.

7.2 Groundwater recharge

Ground water recharge is the component of the water balance on which we pay the most attention and spend the most of the time modelling because its reliable estimation is the final goal of this study. During the calibration phase, we want the simulated annual groundwater recharge to fit with a theoretical values coming from the Guttman and Zukerman formula for estimation of replenishment of the aquifer in function of precipitation (Guttman& Zukerman 1995).

As written before, natural groundwater recharge is function of precipitation along with many other factors; lot of different authors tried to identify empirical correlations between recharge and precipitation; the one by Guttman & Zukerman (1995) was already successfully used in Israel and calculates the replenishment using three different equations depending on the intensity of the rain. The complete formula is the following:

$$R = 0.8 \times (P - 360) \quad if \;\; P > 650mm$$
$$R = 0.534 \times (P - 216) \quad if \;\; 300 < P < 650mm$$
$$R = 0.15 \times P \quad if \;\; P < 300mm$$

Where R is the annual recharge and P is the total annual precipitation.

This formula enables one to calculate annual groundwater recharge; the third equation was the most used in this case because it describe the replenishment from rainfall lower than 300 mm which usually takes place only during rainstorms, where lot of rain fall in short period of time, and this is the typical behavior of this area. The coefficient which correlate precipitation to recharge is so small (relative to the others two) because during rainstorms there is high probability for some of the water to become surface runoff and don't participate to ground water replenishment

Values of daily groundwater recharge simulated by the model were sum each year in order to obtain annual yearly ground water recharge, so they were compared with the values calculated by the theoretical formula, also in yearly time step (figure 7.5).

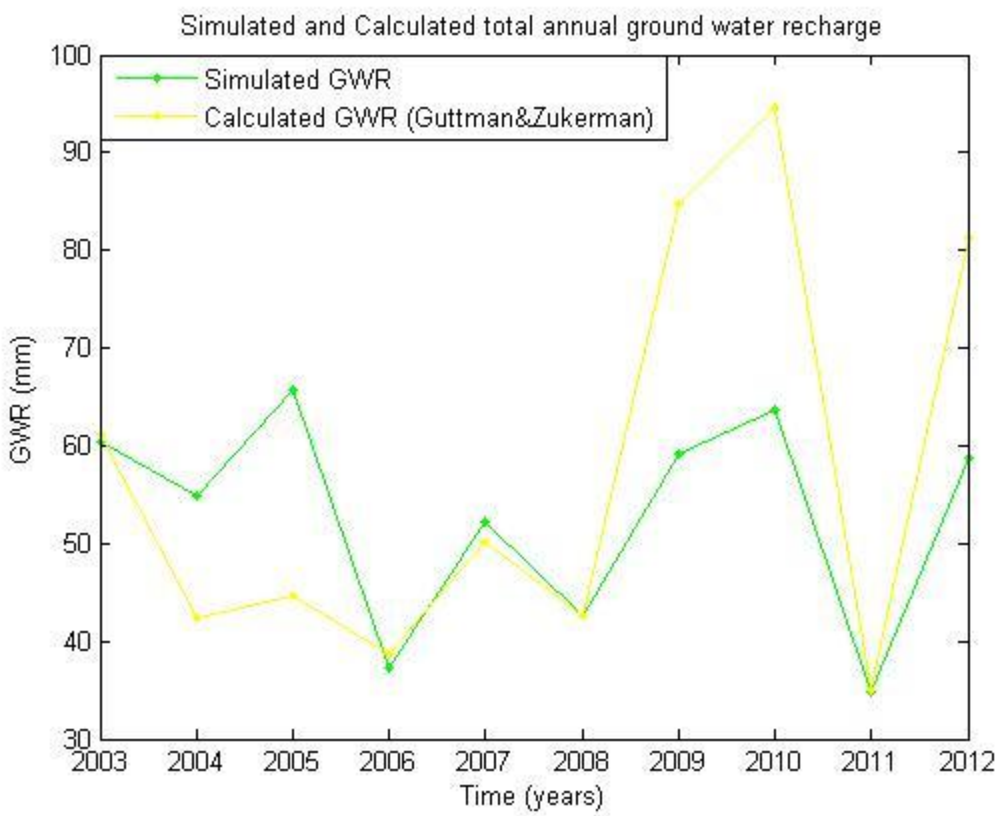

Figure 7.5. Comparison between total annual ground water recharge simulated by the model and calculated with Guttman and Zukerman's formula. The best fit is observed in the period 2006-2008 and also for the years 2003 and 2011. The maximum error occurs in 2010.

In the following picture is shown the absolute maximum error for each year (figure 7.6). Variability of the error is quite high; it goes from almost zero in the year 2008 to about 30 mm in the year 2010.

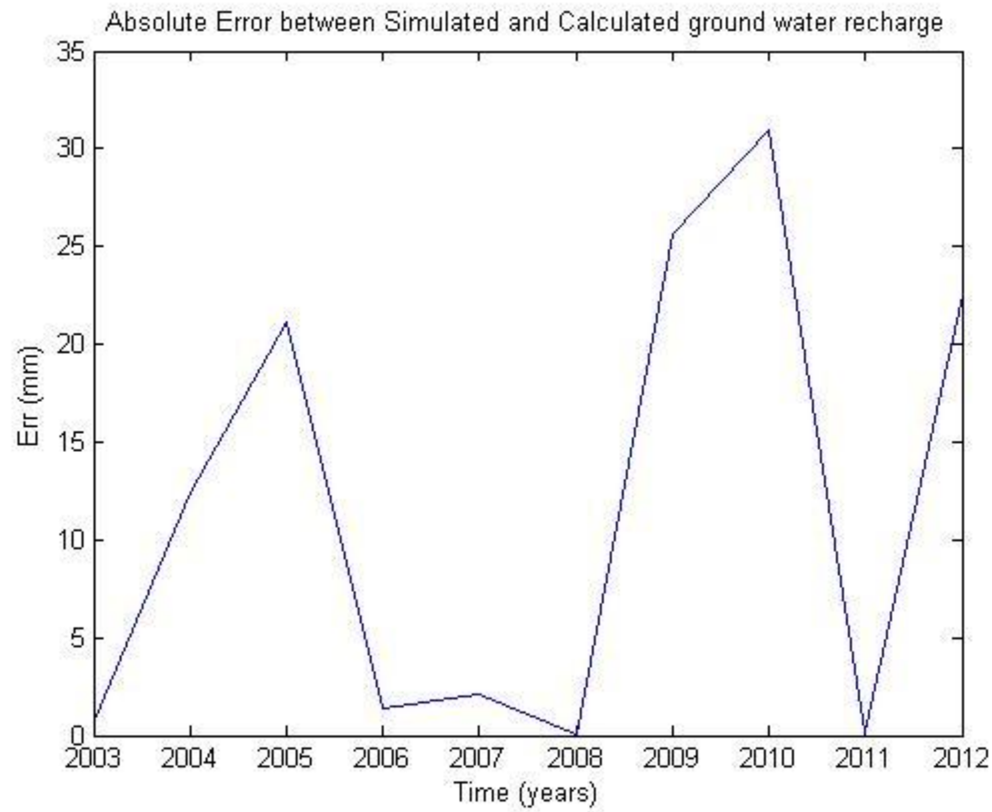

Figure 7.6. Absolute error between simulated and calculated groundwater recharge in the phase of calibration

In table (7.7) are shown the result of the three efficiency function utilized for evaluating the fitting of the model with the Guttman and Zukerman curve in the calibration phase. The mean annual groundwater recharge for the all period differs from the simulated one of only 4.57 mm.

Simulated and Calculated (Guttman&Zukerman) Total Annual Groundwater Recharge - Efficiency

	NSE	**Err Rel**	**R^2**
Value	0.3541	0.1766	0.4238

Table 7.7. Values of Nash-Sutcliffe efficiency (NSE), Relative mean error (Err Rel) and Squared Correlation Coefficient (R^2) obtained, in the calibration phase, comparing groundwater recharge simulated by J2000g with the one calculated with Guttman and Zukerman's formula.

In addition to the comparison of the two curves, the trend of groundwater recharge respect to the amount of rain that generated it was compared, in both cases. If the model prediction is good, the trend should be the same, and in general it should follow the rule that as much rain fall in the catchment as much groundwater recharge we should observe. The following picture (figure 7.8) show Annual groundwater recharge calculated by Guttman & Zukerman with its correspondent annual rain:

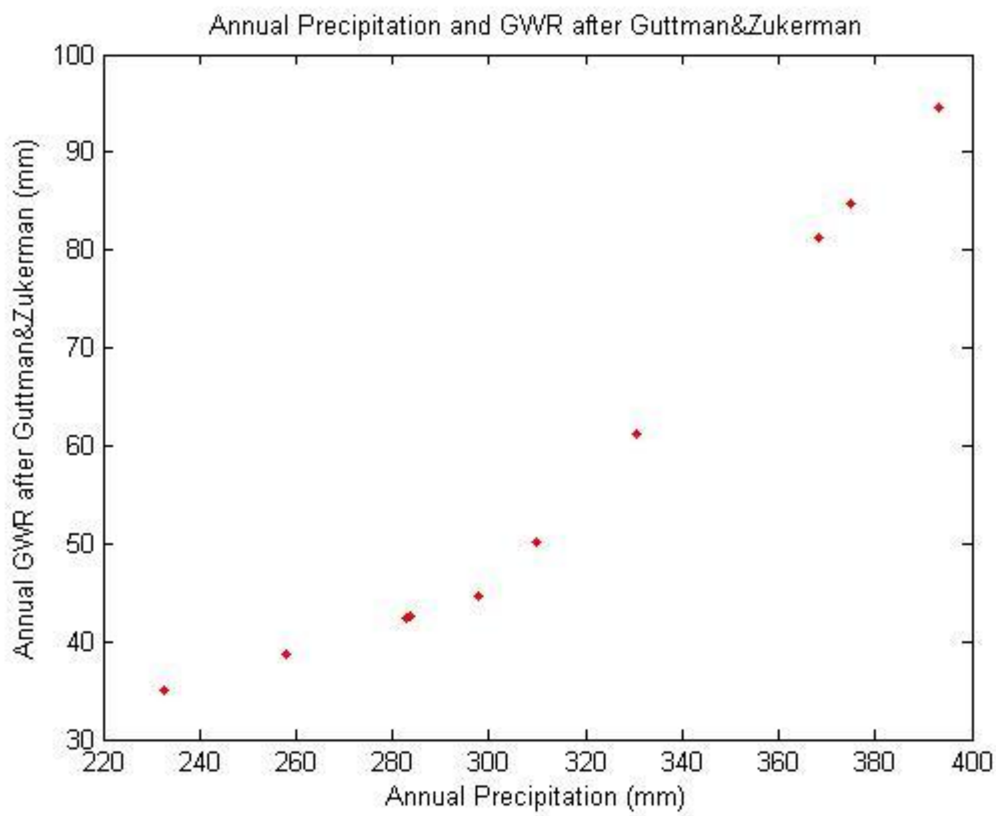

Figure 7.8. Comparison between annual precipitation and annual groundwater recharge after Guttman & Zukerman, the trend reflect the dynamic of the real phenomenon of groundwater recharge: the maximum of recharge is observed when there is the maximum of precipitation.

We compared this trend with the one observed comparing monthly precipitation with monthly groundwater recharge calculated by the model J2000g, showed in figure 7.9:

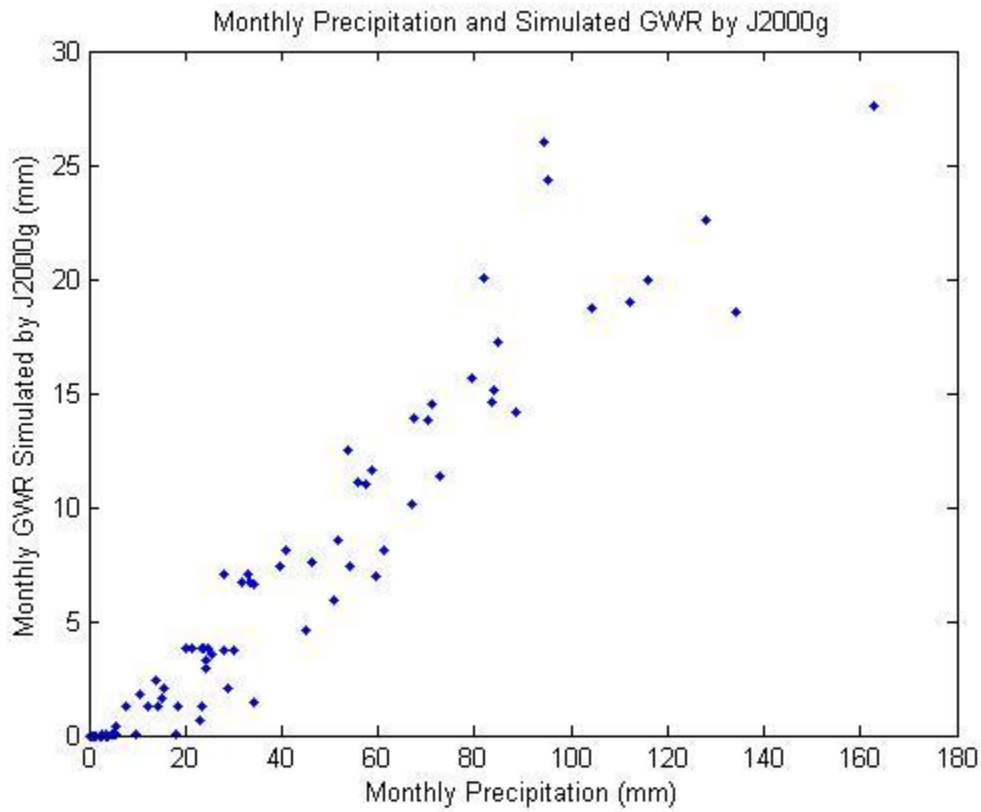

Figure 7.9. Comparison between monthly precipitation and monthly groundwater recharge simulated by the model J2000g: the trend shown is similar to the one after Guttman & Zukerman.

Of course in the monthly time step there are twelve times more values then in the yearly one, but is easily observable that the trend is almost the same. Also changing the time step from monthly to weekly the trend is still quite conserved (figure 7.10):

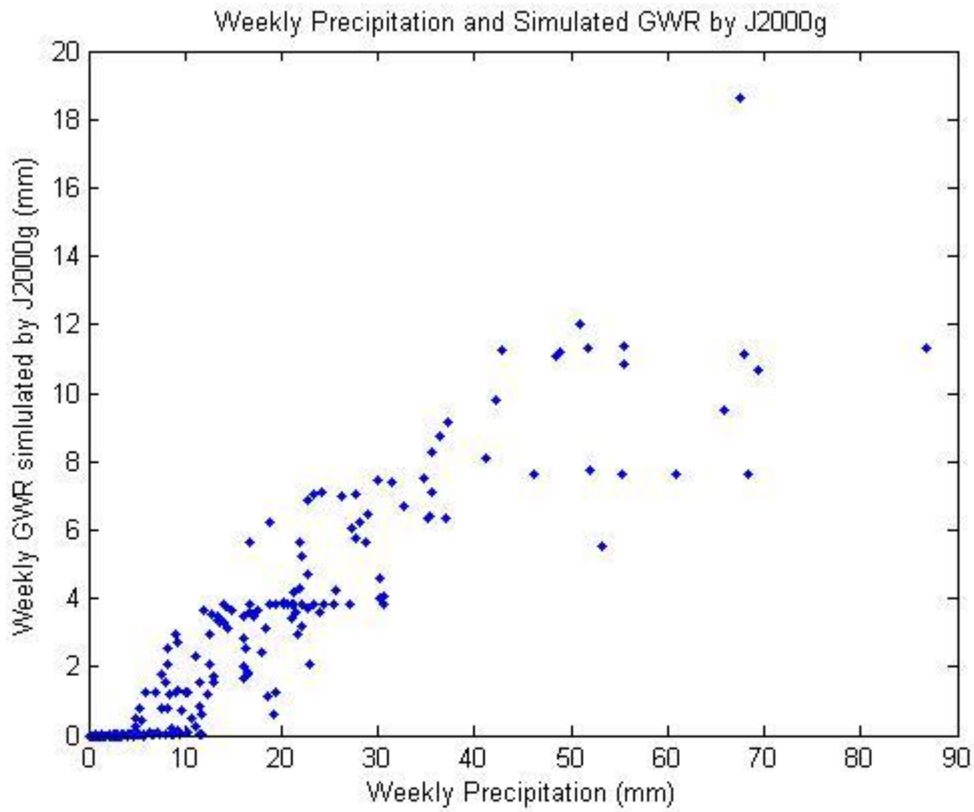

Figure 7.10. Comparison between weekly precipitation and weekly groundwater recharge simulated by the model J2000g: the trend is still quite the same of the two graphics above and, in addition, it shows that not all the amount of water generate groundwater recharge.

From this last plot is evident another important characteristic of this phenomenon: not all the amount of rain generates groundwater recharge. Rain below 5 mm doesn't generate any water storage.

In the validation phase, simulated GWR was compared with GWR estimated by the Chloride Mass Balance Method (CMBM). In absence of measured values we used two different methods to generate groundwater recharge curves for calibrating and validating the model. The two curves show similar trends and values and this make us sure about their reliability. In particular, Chloride mass-balance come from measured values (precipitation and chloride concentrations were measured in field) so it can be considered as a measured value having high reliability.

7.3 Runoff

The runoff plot coming from the model cannot be compared with any source of data because of the absence of measured values. The few hourly data available for some events at the catchment outlet of the catchment were integrated using Origin Pro to generate 42 daily values. Only in these days we checked if the model prediction was right or not. We used two different efficiency criteria: we checked if when runoff occurs in measured values it occurs also in the simulated ones, and then we analyzed the non-zero values more in detail introducing a tolerance value between measured and simulated values out of whom the prediction is considered wrong. In most cases simulated runoff was higher than measured runoff and that means there is too much water in the system. Thus, when ET and GWR are fitted well runoff is usually high. But runoff data are less reliable because the events that occur in this area are usually too fast to be adequately captured and described by a daily model. Here, runoff events mostly occur as flash floods, having runoff amounts of up to 5 m^3/s for a few minutes or one hour. But when averaging these flash flood events to daily time scales discharge does not exceed 40 l/s.

8. VALIDATION AND EFFICIENCY

The validation strategy is based on the goodness of groundwater recharge prediction, as that is what we want the model to accurately predict. As said before, we calibrate the model with particular attention to the groundwater recharge component, the simulated curve was compared with the theoretical formula from Guttman and Zukerman, which was already successfully used in Israel (Guttman et al., 1995); we tried to fit the simulated curve as much as possible with the calculated ones. The validation is made comparing the curve with the chloride mass-balance one to check if the prediction was good.

8.1 Groundwater recharge estimation using Chloride mass-balance

Groundwater recharge is "the movement of moisture downwards through the unsaturated zone to the saturated one" (Freeze & Cherry, 1979) and it represents the main source of fresh water is in West Bank. A reliable estimation of this variable is a challenge of fundamental importance in order to allow a wise water resource management and protection in this area. The quantity of replenishment is function not only of meteorological input but also of geological structure of the aquifer along with many other factors such as vegetation, land use, topography etc. The chloride mass-balance was already successfully used in West Bank to estimate recharge rate (Marei et al., 2010) and therefore it can be considered to be a good means for validation while checking the accuracy of the model in groundwater recharge prediction.

Chloride mass-balance consists in estimate ground water recharge in function of precipitation, concentration of chloride in rain and concentration of chloride in groundwater. Chloride is soluble, conservative and not absorbed by vegetation, that's make it suitable to be used as environmental tracer for groundwater recharge estimation; moreover the method is rapid and inexpensive because of the simple data requirement. The formula used is the following:

$$R = P \times \frac{Cl_p}{Cl_{gw}}$$

where R is recharge (mm/year), P is rainfall (mm/year), Cl_p is weighted average chloride concentration in rainfall (mg/l) and Cl_{gw} is average chloride concentration in groundwater (mg/l)

Even though the method can satisfactorily describe the dynamic of the phenomenon in this area, it is still a simplification of the reality, so its implementation needs some preliminary assumptions:

- additional sources of chloride coming from dissolution of minerals are neglected (wastewater etc.),
- chloride is totally conservative in the system, that means it is not absorbed and it does not participate to any chemical reaction,
- there is no groundwater evaporation (groundwater table is assumed deep enough to prevent this phenomenon)
- the magnitude of surface runoff is limited

The first assumption does not reflect the reality because absence of chloride sources in this area is impossible: there is wastewater from the upper mountains communities and the geology is composed by lot of salty rocks, which means the excess of chloride is not ignorable. The chloride excess is taken into account by using the Br/Cl molar ratio in both rain and groundwater chloride concentration to calculate additional quantity of chloride, in this area the value suggested for the ratio is 300 (Rosenthal, 1987) and the excess of chloride ranges between 15 and 20% of the measured value. All of the following values have been already reduced from the chloride excess.

The second assumption is also not totally true but it can be assumed to be valid because the amount of chloride absorbed by vegetation is usually balanced by the amount released by plants decomposition (Edmunds et al., 1988).

Third and fourth assumptions can be considered to be in good agreement with the reality in this area, especially the one of minimal surface runoff.

Iin October 2012 scientists of UFZ performed a field trip in Israel and sampled chloride concentration in groundwater; measurements in two different stations in Darga catchment are available, Jerusalem 6 and Al Azaria 1, and they show a chloride concentration of 55.2 mg/l and 22.7 mg/l respectively, the medium values from this two is taken as average value for the catchment and used as Cl_{gw} in the formula. For the chloride concentration in rainfall values from samplings in Hizma Jerusalem are taken (Marei et al., 2010) and Cl_p is calculated as

$$Cl_p = \frac{P1 \times C1 + P2 \times C2 + \cdots + Pn \times Cn}{P1 + P2 + \cdots + Pn}$$

Where, for every event from 1 to *n*, *Pn* (mm) is the rainfall of the event and *Cn* (mg/l) is the corresponding chloride concentration in the rainfall. The amount of water for every event is multiplied by his correspondent chloride concentration, then all this components are summarized and the sum is divided by the total water amount of all the events.

Flowing there is the comparison between simulated ground water recharge and calculated with Chloride mass-balance (Figure 8.1); the absolute error is shown in figure 8.2 and it can reach at least 14 mm in 2005, in 2007 can be observed the best prediction of the model with an absolute error of almost zero. Efficiency is evaluated by calculating Nash-Sutcliffe efficiency, Relative Mean Error and coefficient of correlation (table 8.3).

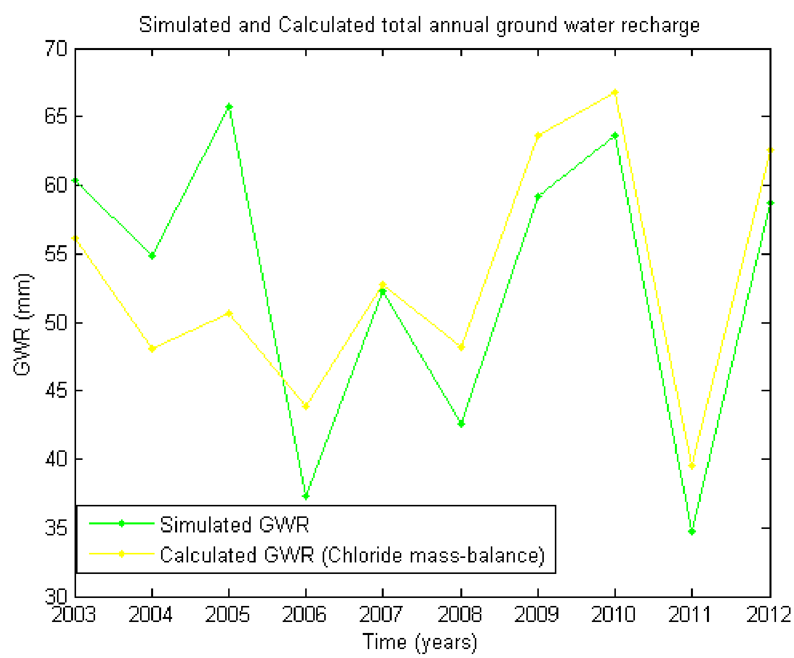

Figure 8.1. Simulated groundwater recharge by J2000g model (green) and calculated groundwater recharge using Chloride mass-balance method (yellow).

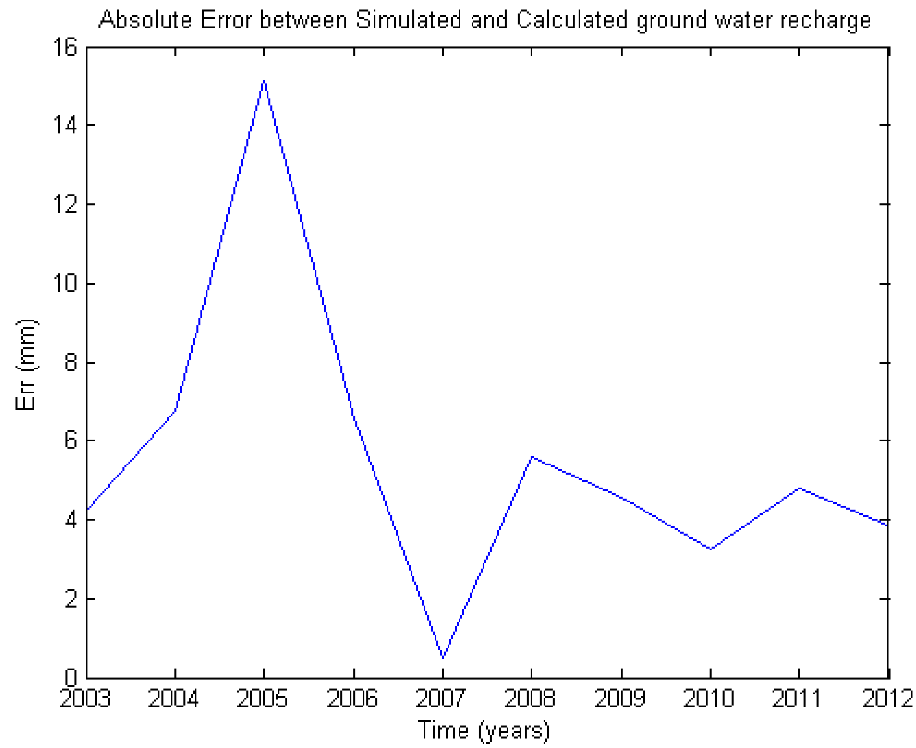

Figure 8.2. Absolute Error in groundwater recharge prediction (respect to Chloride mass-balance).

Efficiency in GWR prediction

	NSE	**Err Rel**	R^2
Value	0.3974	0.1093	0.6026

Table 8.3. Nash-Sutcliffe efficiency, Relative Mean Error and the Squared Correlation Coefficient for groundwater recharge estimation (respect to Chloride mass-balance).

Considering the mean annual ground water recharge (sum of all the values and divided by the number of years), simulated groundwater recharge differs from the one calculated with Chloride mass-balance for only 0,3 mm. That means in the long period the model is really good in groundwater recharge prediction.

The better results with Chloride mass balance respect to the Guttman&Zukerman formula indicate that the prediction is reliable because chloride mass balance comes from measured values and so it is expected to be really more precise and reliable than a theoretical formula.

8.2 Runoff

As said before, runoff cannot be used for calibration because data are not enough to make a realistic comparison; also in the validation phase it cannot be used for estimating the efficiency of the model, that is a limit of prediction in runoff ungauged basin. Anyway, for the sake of completeness, simulated runoff are shown in figure 8.4:

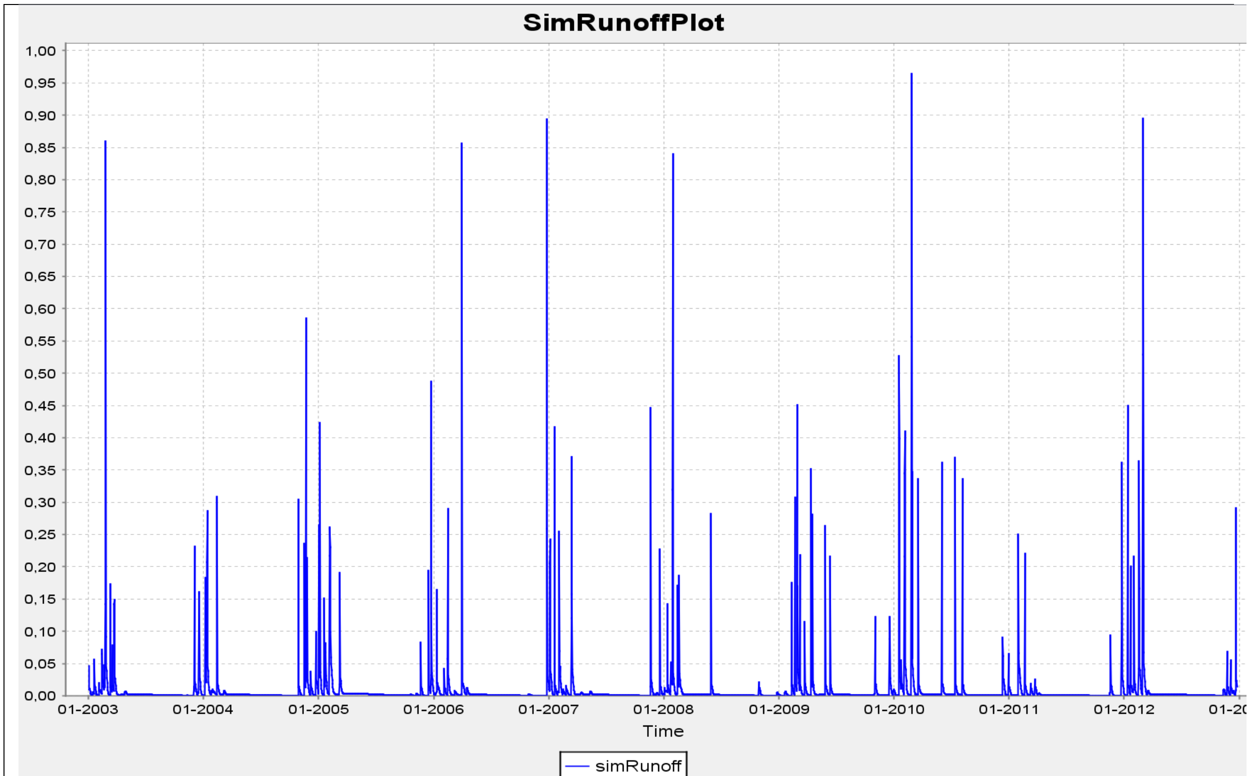

Figure 8.4. Simulated runoff plot (mm/day).

We considered the runoff response of the model only in the 42 days where observed values are available and check out if these values fit with the others. The first step was to count how many days out of this 42 the model can guess right (for each day if both values are 0 or both values are positive the model prediction was considered right). According to this simplification 33 values out of the 42 are considered right.

The second step consists in making a more precise analysis counting as right guess only the days in which the simulated runoff is in the range:

$$ObsRunoff - P \times ObsRunoff < SimRunoff < ObsRunof + P \times ObsRunoff$$

Where P (-) is the tolerance of the gap between observed and simulate runoff. It is inferior limited (zero) but not superior limited. With the chosen of 1 we consider good predict values that can be at least the double of observed runoff. With the chosen of value of 0.5 we accepted that a good value of simulated runoff can be at least 50% more of the correspondent observed runoff, or 50% less, and so on (With the chosen of zero we accept as good right only the values of simulated runoff that are exactly the same to the correspondent observed ones). In this study we considered P=1 and P=0.5, it doesn't make much sense to be stricter, because this few values are not really representative of the goodness of the model prediction and the calibration was not made looking at these values. The aim is only to be sure that the response of the model for this component of the hydrologic cycle was not too far from the reality.

	Days
Number of observed runoff	42
Well predicted values without tolerance	32
Well predicted values with tolerance P=1	21
Well predicted values with tolerance P=0,5	11

As expected, as much the tolerance decrease less values of the simulation are considered good.

9. RESULTS

Model provides spatially distributed output for every hydrological variable of interest. That means in every Hydrological Response Unit (HRU) and for every time step a single value is calculated. For each HRU we first calculated a daily average by summing all the values of all the days of the simulation, and then by dividing this sum by the number of days. After that the daily average in each HRU is multiplied by 365 (number of days in one year) in order to obtain a yearly average. These values are then loaded in ArcGIS and plotted. That was done for Ground water recharge, actual soil moisture, potential and actual evapotranspiration.

Groundwater recharge (figure 9.1): the spatial pattern of groundwater recharge, showing a linear changing from dark blue in the upper catchment to light blue near the outlet, makes sense and it is as expected. It is higher in the highest part of the catchment, where precipitation is higher, and lower in the lowest part of the catchment, where there is small precipitation and arid condition are stronger. After this general trend three zone of high recharge can be observed in the picture. These are the areas characterized by the presence of the geological formation Bina (figure 3.3), which is more permeable than the others formations and contributes a lot in forming groundwater storage. Groundwater recharge occurs mostly in these zones, where it can reach more than 100 mm/year. In the zone of low recharge, near the Dead Sea, the entity of the recharge can be less than 30 mm/year.

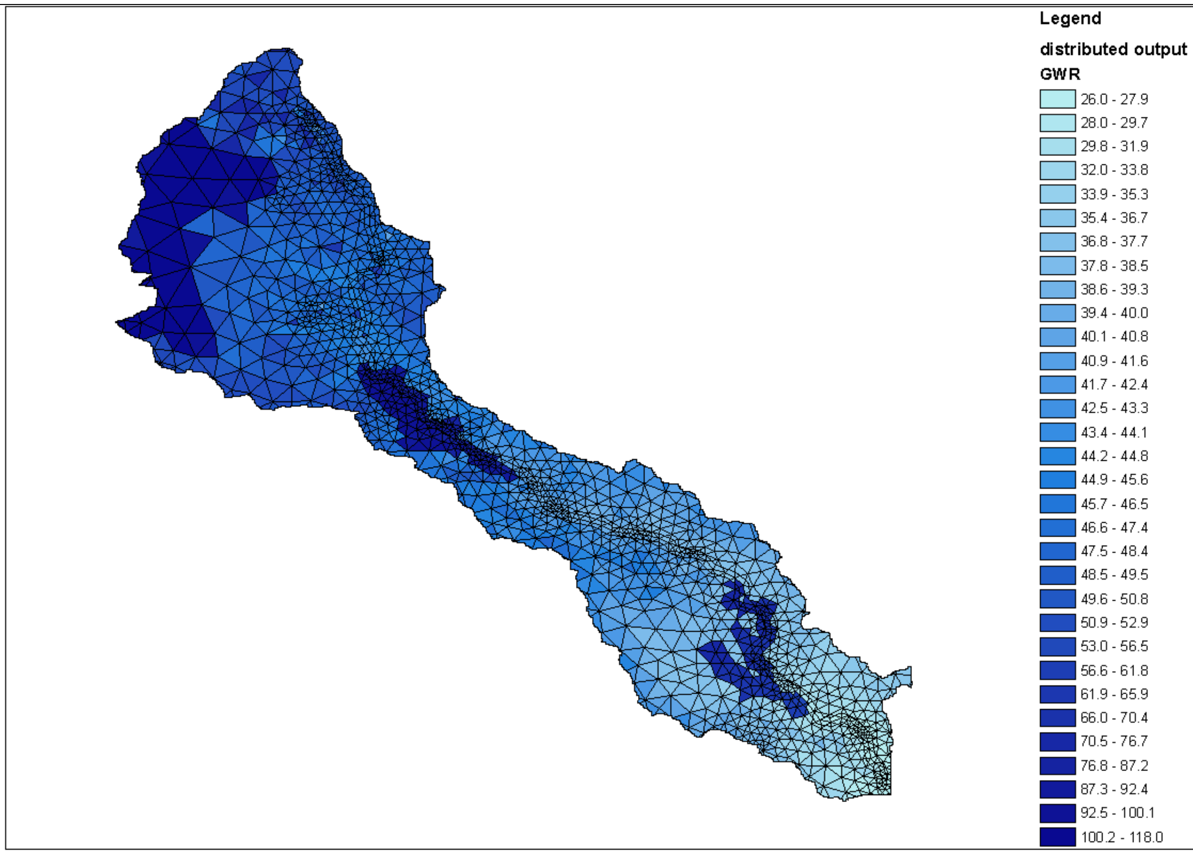

Figure 9.1. Annually spatially distributed Groundwater Recharge (mm).

Soil moisture (figure 9.2): the spatial pattern of soil moisture reflects the availability of water in the catchment. It is higher in the north where more precipitation occurs and lower in the south, as said before, dominated by arid conditions. The range of annual soil moisture goes from 2.8 to 387.7 mm/year

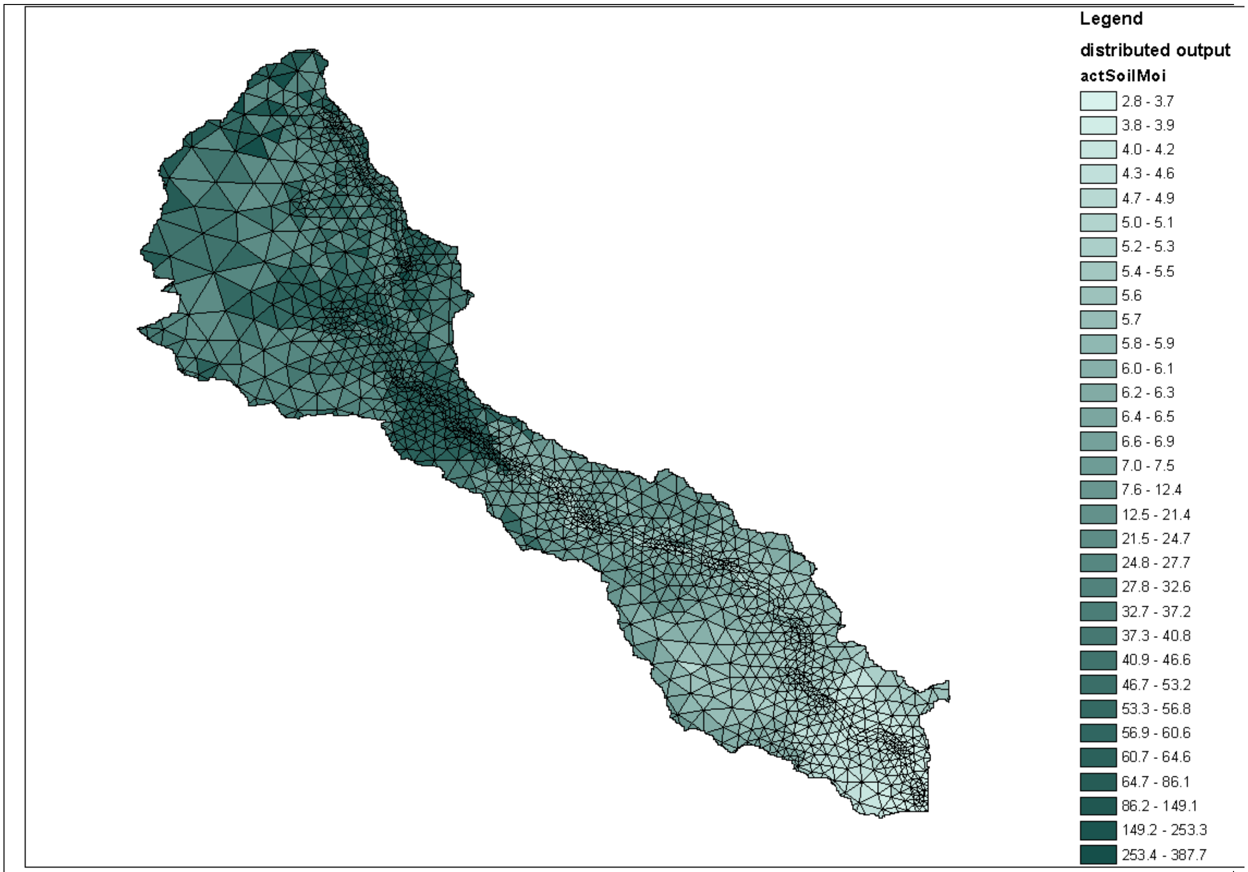

Figure 9.2. Spatially distributed soil moisture (mm/year).

Potential Evapotranspiration (figure 9.3): PET distribution reflects climate condition; it is maximum in the south of catchment, near the Dead Sea, where the arid conditions are stronger and minimum in the north of the catchment where temperature is usually lower. Changing is quiet gradual and the range of values for the annual sum goes from 1780 to more than 3000 mm/year.

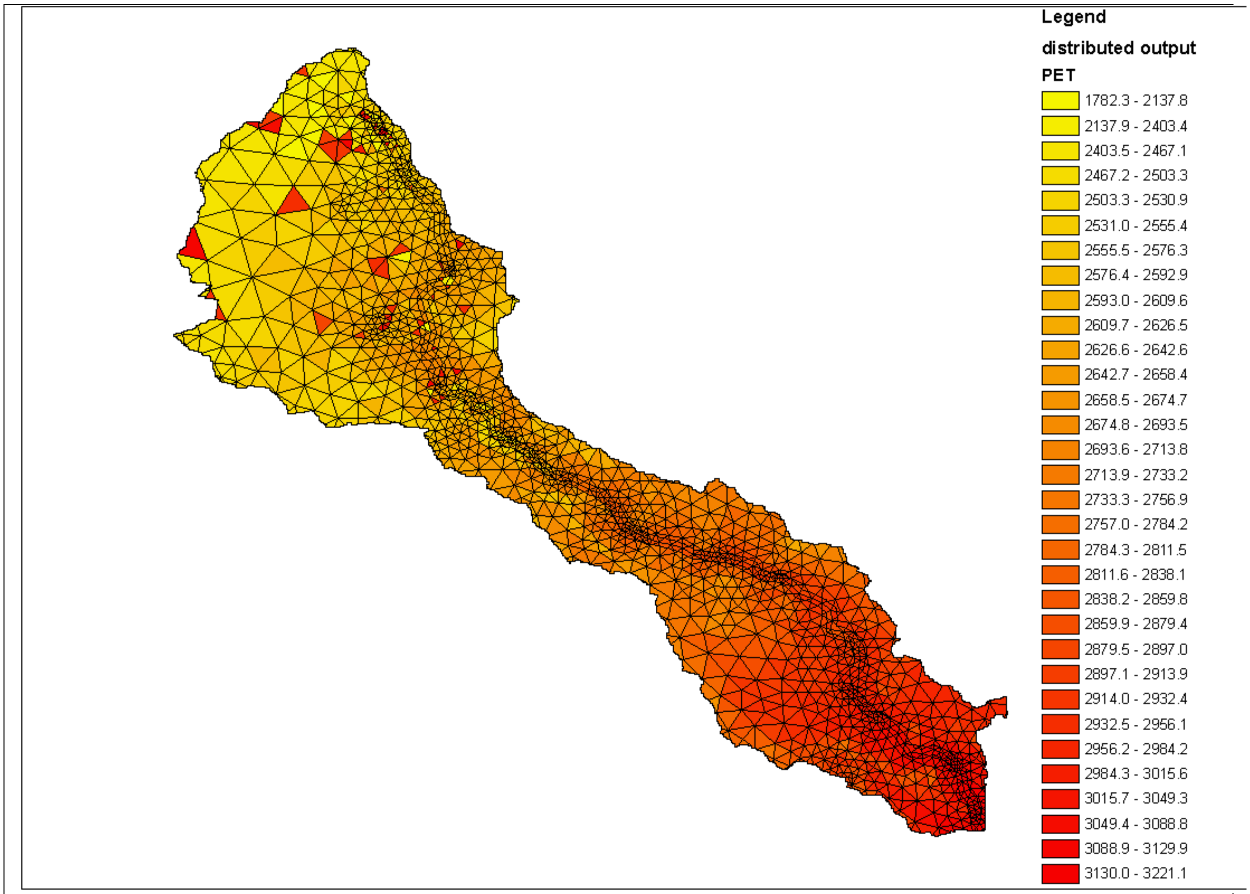

Figure 9.3. Spatially distribution of Potential evapotranspiration (mm/year).

Actual Evapotranspiration (figure 9.4): AET can be limited by water or by the value of PET; as expected, the dominant limitation for AET in this area is the amount of water, because the maximum value of AET (195,5 mm) is inferior to the minimum value of PET (3221,1 mm). AET never reaches the maximum threshold defined by PET and it occurs only where there is availability of water in the catchment. It should occur mostly in the upper side of the catchment because that area is supposed to have most quantity of water, but as we can see in the picture there are high variability and a not precise trend. That occurs because in the calibration phase, in order to obtain a good groundwater recharge, we set the parameter "InitSoilWater.FCAdaptation" to be small, which means most of the water that is not runoff, became groundwater recharge instead of evapotranspiration. So in the upper part of the catchment, where AET should be high, AET is low because most of the water recharges the groundwater storage. Some of the areas with high values of AET coincide with areas of high soil moisture and that reflects well the reality of the natural phenomenon.

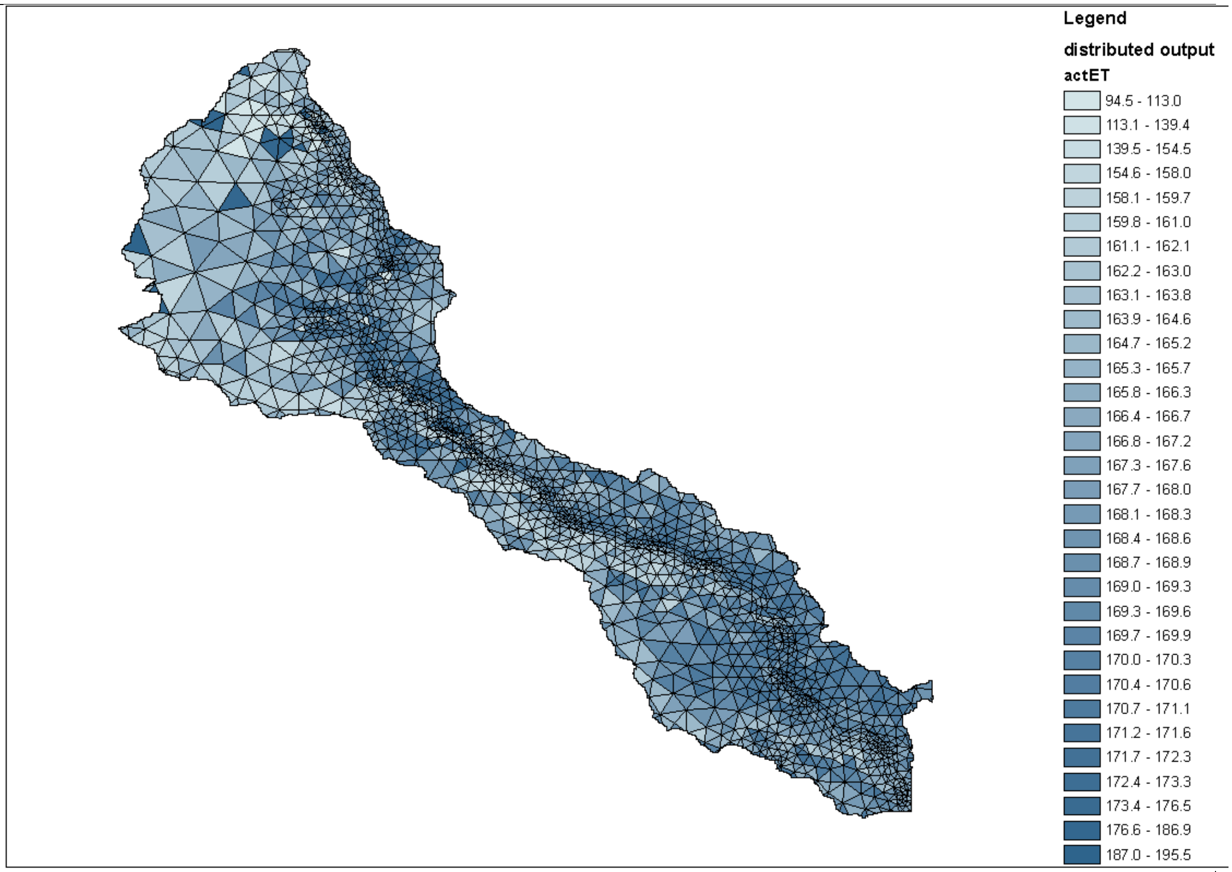

Figure 9.4. Spatially distributed actual evapotranspiration (mm/year).

10. CONCLUSIONS

Water is a valuable resource in areas characterized by water shortage, it cannot be wasted and its correct quantification is a very important and topical hydrological issue. Darga catchment is an arid area in West Bank with groundwater as main water resource; the aim of this work was to estimate is replenishment in a reliable way. We utilized a spatially-distributed conceptually-based hydrological model to estimate groundwater recharge continuously in time and distributed in space. The lack of streamflow data for the study catchment forced us to apply an alternative calibration-validation strategy based on multiple variables and parameters; goodness of model prediction was evaluated by suitable objective functions. In particular, the Dissertation presents some of the possible strategies and solutions to effectively address the problem of estimation of hydrological variables in arid areas and partially ungauged catchments. The most significant problems we had address were (i) the shortage of measured streamflow data and (ii) the difficulty to find reliable literature and satellite data for this area.

Concerning streamflow data, the absence of long hydrometric time series makes it impossible to perform a traditional calibration. The very sparse streamflow observations (i.e. 42 daily values spanning over ten years) was used for a qualitative validation, in order to be sure that the model output did not differ significantly from the observations.

Concerning evapotranspiration we referred to Modis values of potential evapotranspiration (PET) to test the energy balance simulated by the model.

Actual evapotranspiration from satellite data was found to be not reliable. We compared in the study two different satellite AET datasets and they resulted to be very different from each other, also they showed a really small variability between summer and winter seasons, with high values in summer months, which does not make sense since the catchment is generally dry in that period. We computed actual evapotranspiration through the model as a function of reliable values of PET and soil moisture, and therefore we are confident that AET estimates are reasonable. However we do not have measured values to compare simulated daily AET series against.

The model was found to correctly simulate ground water recharge under a correct calibration, it estimates an annual groundwater recharge of 52,9 mm/year, which is the same estimated by chloride mass-balance (53,2 mm/year). The choice of daily time step was mandatory in our case, because of the absence of input data at a finer temporal resolution. Nevertheless, daily timescale was not found to be the best to represent the dynamics of the complex hydrological system and the natural water cycle in the study area. The aridity conditions, in fact, usually generate long interstorm periods (time period without rain) interrupted by very short and intense thunderstorms. The resulting fast runoff, usually called flashflood, cannot be well described by a daily temporal scale.

Future improvements of this work, which aim at improving the modeling accuracy, would start with a collection of measured data for longer time periods and for different variables, in order to be able to:

- Perform a standard calibration-validation strategy, based on the comparison of simulated and observed runoff (as well as other hydrological variables) series;
- Compare results such as actual evapotranspiration and soil moisture with real values instead of literature or satellite values;
- Validate the model for a time periods that is longer than the one used for calibration.

APPENDIX: Matlab's scripts

A.1 Aridity index Calculation

The script calculates aridity index. The input values are daily Potential Evapotranspiration and Precipitation.

```
% Calculation of aridity
clc
clear all
close all

filename =
'Y:\Gruppen\na_osten\Alessandro\work\JAMS\AlessandroDarga\output\current\re
sult-gb.dat';
DELIMITER = '\t';
HEADERLINES = 3; %J2000g output

% Import the file
All = importdata(filename, DELIMITER, HEADERLINES);
% Read 1 column
PETJ2000g = All.data(:,12); % PET calculated according to Penman Method
Rain = All.data(:,1); % precipitation

PET=mean(PETJ2000g);
PREC=mean(Rain);

Aridity=PREC/PET
```

A.2 Chloride Mass-Balance implementation

The script implements Chloride Mass-Balance method. Input variables are Precipitation and chloride concentrations in rainwater and groundwater. Groundwater recharge is calculated as function of precipitation and chloride concentrations and plotted together with simulated groundwater recharge. Script calculates values of Nash-Sutcliffe efficiency, Relative Mean Error and R^2.

```
%CHLORIDE MASS-BALANCE
clc
clear all
close all
filename =
'Y:\Gruppen\na_osten\Alessandro\work\JAMS\AlessandroDarga\output\current\re
sult-gb.dat';
DELIMITER = '\t';
HEADERLINES = 3;

% Import the file
All = importdata(filename, DELIMITER, HEADERLINES);
% Read 1 column
SimGWR = All.data(:,18); %read gwRecharge from result-gb
SimRain = All.data(:,1);  %read precip from result-gb

TASGWR03=sum(SimGWR(1:363));  %Total Annual Simulated GWR year 2003
TASGWR04=sum(SimGWR(364:729));
TASGWR05=sum(SimGWR(730:1094));
TASGWR06=sum(SimGWR(1095:1459));
TASGWR07=sum(SimGWR(1460:1824));
TASGWR08=sum(SimGWR(1825:2190));
TASGWR09=sum(SimGWR(2191:2555));
TASGWR10=sum(SimGWR(2556:2920));
TASGWR11=sum(SimGWR(2921:3285));
TASGWR12=sum(SimGWR(3286:end));

TASGWR=[TASGWR03 TASGWR04 TASGWR05 TASGWR06 TASGWR07 TASGWR08 TASGWR09
TASGWR10 TASGWR11 TASGWR12]';
Mean_Annual_Sim_GWR=mean(TASGWR) %mean annual simulated ground water
recharge

TASR03=sum(SimRain(1:363));  %Total Annual Simulated Precipitation year
2003
TASR04=sum(SimRain(364:729));
TASR05=sum(SimRain(730:1094));
TASR06=sum(SimRain(1095:1459));
TASR07=sum(SimRain(1460:1824));
TASR08=sum(SimRain(1825:2190));
TASR09=sum(SimRain(2191:2555));
TASR10=sum(SimRain(2556:2920));
TASR11=sum(SimRain(2921:3285));
TASR12=sum(SimRain(3286:end));
```

```
TASR=[TASR03 TASR04 TASR05 TASR06 TASR07 TASR08 TASR09 TASR10 TASR11
TASR12]';

%calculation of Annual GWR with Chloride mass-balance
CLp=6.62; %chloride concentration in rainwater of Hizma Jerusalem [mg/l]
CLgw=38.95; %average chloride concentration in ground water of Darga
CGWR=TASR*CLp/CLgw; %Annual Ground water Recharge

Mean_Annual_calc_GWR=mean(CGWR) %mean annual calculated ground water
recharge

%Difference between calculated and simulated mean annual gwr
difference=abs(Mean_Annual_calc_GWR-Mean_Annual_Sim_GWR)

t=[2003:1:2012];   %years from 2003 to 2012
figure;
plot(t,TASGWR,'.-g',t,CGWR,'.-y')
title('Simulated and Calculated total annual ground water recharge');
xlabel('Time (years)');
ylabel('GWR (mm)');
legend('Simulated GWR','Calculated GWR (Chloride mass-balance)')

%Absolute Error: calculation of the difference between calculate and
simulate GWR
   for i=1:length(CGWR)
       ERR_VOL(i)=abs(TASGWR(i)-CGWR(i)); %error of each year
   end
   ERR_VOL=ERR_VOL';

figure;
plot(t,ERR_VOL)
title('Absolute Error between Simulated and Calculated ground water
recharge')
xlabel('Time (years)');
ylabel('Err (mm)');


% Nash-Sutcliffe efficiency NSE

MeanCGWR=mean(CGWR); %average value of the vector CGWR

for i=1:length(CGWR)
    A(i)=(TASGWR(i)-CGWR(i))^2;

    B(i)=(CGWR(i)-MeanCGWR)^2;

end
 A2=sum(A);
 B2=sum(B);

NSE=1-A2/B2

%Relative Mean Error
```

```
for i=1:length(CGWR)
    if CGWR(i)~=0
    e(i)=(abs(TASGWR(i)- CGWR(i)))/CGWR(i);
    end
end
    E=sum(e);
    Err_rel=E/numel(CGWR);


% R2
Corr=corr2(TASGWR,CGWR)^2;

% Result table
f=figure('Position', [300 500 700 160]);
title('Efficiency in the prediction of GWR')
cnames={'NSE','Err Rel','R^2'};
rnames={'value'};
tabella(:,1)=NSE;
tabella(:,2)=Err_rel;
tabella(:,3)=Corr;
t=uitable('Parent',f,'Data',tabella,'Position',[20 20 650
120],'ColumnName',cnames,'RowName',rnames);
```

A.3 Daily Actual Evapotranspiration

The script reads data of Actual Evapotranspiration from an excel file (values are expressed as 8-days sum according to Julian calendar), divides them by 8 to obtain daily values and sets each value for 8 days.

```
clear all
clc

data=xlsread('Y:\Gruppen\na_osten\Alessandro\work\JAMS\PET\scripts\MeanAET'
);

data = data/8;

a=1;
for i=1:numel(data)             %reads data of every 6th row (LAI_1km in
MODIS MOD15A2 dataset)
    for j=1:8           %writes 8-day entry to 8 single day entries
    AET(a,:) = data(i);
    a=a+1;
    end
end
```

A.4 Actual and Potential Evapotranspiration

Script compares Potential Evapotranspiration simulated by the model with the one from satellite data and calculates Nash-Sutcliffe efficiency, Relative Mean Error and R^2. Same plot and calculation is done for values of Actual Evapotranspiration and in the last plot soil moisture is added.

```
% Comparison between potET from Model J2000g and PET from MODIS
% DATABASE
clc
clear all
close all

filename =
'Y:\Gruppen\na_osten\Alessandro\work\JAMS\AlessandroDarga\output\current\re
sult-gb.dat';
DELIMITER = '\t';
HEADERLINES = 3; %J2000g output

% Import the file
All = importdata(filename, DELIMITER, HEADERLINES);
% Read 1 column
PETJ2000g = All.data(:,12);

nJ=length(PETJ2000g);

load('PET_avg.mat');

nM=length(PETspatial_avg);
if nM>nJ    %if PETspatial_avg has more values than PETJ2000g
PETspatial_avg(nJ+1:end)=[];
else
    PETJ2000g(nM+1:end)=[];
end

PETmodis=PETspatial_avg;

T=1:min(nM,nJ);
T=T';

figure;
plot(T,PETmodis,'-r',T,PETJ2000g,'-g')
title('Potential ET from Modis and J2000g');
xlabel('Time (Days)');
ylabel('PET (mm)');
legend('Modis PET','Model PET')

%Absolute Error: calculation of the difference between PETmodis and
%PETJ2000g
```

```
   for i=1:length(PETmodis)
       ERR_VOL(i)=abs(PETmodis(i)-PETJ2000g(i)); %error of each year
   end
   ERR_VOL=ERR_VOL';
   ERR_VOL_mean= mean(ERR_VOL)


%Nash-Sutcliffe efficiency NSE

MeanM1=mean(PETmodis); %average value of Modis PET

for i=1:length(PETJ2000g)
    C(i)=(PETJ2000g(i)-PETmodis(i))^2;

    D(i)=(PETmodis(i)-MeanM1)^2;

end
 C2=sum(C);
 D2=sum(D);

NSE_PET=1-C2/D2
%%
% Comparison between J2000g's actET and AET from MODIS DATABASE

filename =
'Y:\Gruppen\na_osten\Alessandro\work\JAMS\AlessandroDarga\output\current\re
sult-gb.dat';
DELIMITER = '\t';
HEADERLINES = 3; %J2000g output

% Import the file
All = importdata(filename, DELIMITER, HEADERLINES);
% Read 1 column
AETJ2000g = All.data(:,13);
J=length(AETJ2000g);

load('AET_db8.mat'); %AET divided by 8
M=length(AET);
if M>J
AET(J+1:end)=[];
else
    AETJ2000g(M+1:end)=[];
end

AETmodis=AET;
AETmodis=AETmodis';
AETJ2000g=AETJ2000g';

t=1:min(M,J);
t=t';
T=length(t);
% import and plot Soil Moisture (ACTMPS-> actual middle sized pore storage)
SM = All.data(:,16); %import ACTMPS from result-gb
H=length(SM);
```

```
if H>T % if SM has more values than the other two vectors (AETJ2000g and
AETmodis)
    SM(T+1:end)=[];
end
SM=SM';

figure;
plot(t,AETmodis,'-r',t,AETJ2000g,'-g',t,SM,'-b')
title('Actual ET from Modis and J2000g and Soil Moisture');
xlabel('Time (Days)');
ylabel('AET (mm)');
legend('Modis AET','Model AET','Soil Moisture')

figure;
plot(t,AETmodis,'-r',t,AETJ2000g,'-b')
title('Actual ET from Modis and J2000g');
xlabel('Time (Days)');
ylabel('AET');
legend('Modis AET','Model AET')

% Nash-Sutcliffe efficiency NSE

MeanM=mean(AETmodis); %average value of Modis Actual ET

for i=1:length(AETJ2000g)
    A(i)=(AETJ2000g(i)-AETmodis(i))^2;

    B(i)=(AETmodis(i)-MeanM)^2;

end
 A2=sum(A);
 B2=sum(B);

NSE=1-A2/B2;


%Relative Mean Error

for i=1:length(AETJ2000g)
    if AETmodis(i)~=0
    e(i)=(abs(AETJ2000g(i)- AETmodis(i)))/AETmodis(i);
    end

end
    E=sum(e);
    Err_rel=E/numel(AETJ2000g);

% R2

Corr=corr2(AETJ2000g,AETmodis)^2;

% Result table

f=figure('Position', [300 500 700 160]);
```

```
title('Efficiency in the prediction of AET')
cnames={'NSE','Err Rel','R^2'};
rnames={'value'};
tabella(:,1)=NSE;
tabella(:,2)=Err_rel;
tabella(:,3)=Corr;
t=uitable('Parent',f,'Data',tabella,'Position',[20 20 650
120],'ColumnName',cnames,'RowName',rnames);
```

A.5 Groundwater Recharge

Script compares calculated groundwater recharge according to *Guttman & Zukerman* with the one simulated by model. It also calculates values of Nash-Sutcliffe efficiency, Relative Mean Error and R^2, and plots precipitation, with different time-steps, against the two series of ground water recharge.

```
%Groundwater recharge comparison
clc
clear all
close all
filename =
'Y:\Gruppen\na_osten\Alessandro\work\JAMS\AlessandroDarga\output\current\re
sult-gb.dat';
DELIMITER = '\t';
HEADERLINES = 3;

% Import the file
All = importdata(filename, DELIMITER, HEADERLINES);
% Read 1 column
SimGWR = All.data(:,18); %read the column gwRecharge from result-gb
SimRain = All.data(:,1);  %read the column precip from result-gb

TASGWR03=sum(SimGWR(1:363));  %Total Annual Simulated GWR year 2003
TASGWR04=sum(SimGWR(364:729));
TASGWR05=sum(SimGWR(730:1094));
TASGWR06=sum(SimGWR(1095:1459));
TASGWR07=sum(SimGWR(1460:1824));
TASGWR08=sum(SimGWR(1825:2190));
TASGWR09=sum(SimGWR(2191:2555));
TASGWR10=sum(SimGWR(2556:2920));
TASGWR11=sum(SimGWR(2921:3285));
TASGWR12=sum(SimGWR(3286:end));

TASGWR=[TASGWR03 TASGWR04 TASGWR05 TASGWR06 TASGWR07 TASGWR08 TASGWR09
TASGWR10 TASGWR11 TASGWR12]';
Mean_Annual_Sim_GWR=mean(TASGWR) %mean annual simulated ground water
recharge

TASR03=sum(SimRain(1:363));  %Total Annual Simulated Precipitation year
2003
TASR04=sum(SimRain(364:729));
TASR05=sum(SimRain(730:1094));
TASR06=sum(SimRain(1095:1459));
TASR07=sum(SimRain(1460:1824));
TASR08=sum(SimRain(1825:2190));
TASR09=sum(SimRain(2191:2555));
TASR10=sum(SimRain(2556:2920));
TASR11=sum(SimRain(2921:3285));
TASR12=sum(SimRain(3286:end));
```

```
TASR=[TASR03 TASR04 TASR05 TASR06 TASR07 TASR08 TASR09 TASR10 TASR11
TASR12]';

%calculation of Annual GWR with the formula after Guttman&Zukerman (1995)

for i=1:length(TASR)
    if TASR(i)>650
        CGWR(i)=(0.8*TASR(i)-360);
    else
        if TASR(i)>300
            CGWR(i)=0.534*(TASR(i)-216);
        else

            CGWR(i)=0.15*TASR(i);
        end
    end
end
   CGWR=CGWR'; %Calculate Ground water recharge values from 2003 to 2012
   Mean_Annual_calc_GWR=mean(CGWR) %mean annual calculated ground water
recharge (Guttman&Zukerman, 1995)

difference=abs(Mean_Annual_calc_GWR-Mean_Annual_Sim_GWR) %Difference
between calc and sim mean annual gwr

t=[2003:1:2012];   %years from 2003 to 2012
figure;
plot(t,TASGWR,'.-g',t,CGWR,'.-y')
title('Simulated and Calculated total annual ground water recharge');
xlabel('Time (years)');
ylabel('GWR (mm)');
legend('Simulated GWR','Calculated GWR (Guttman&Zukerman)')

%Absolute Error: calculation of the difference between calculate and
simulate GWR
   for i=1:length(CGWR)
       ERR_VOL(i)=abs(TASGWR(i)-CGWR(i)); %error of each year
   end
   ERR_VOL=ERR_VOL';

figure;
plot(t,ERR_VOL)
title('Absolute Error between Simulated and Calculated ground water
recharge')
xlabel('Time (years)');
ylabel('Err (mm)');

% Nash-Sutcliffe efficiency NSE

MeanCGWR=mean(CGWR); %average value of the vector CGWR

for i=1:length(CGWR)
    A(i)=(TASGWR(i)-CGWR(i))^2;

    B(i)=(CGWR(i)-MeanCGWR)^2;
```

```
end
 A2=sum(A);
 B2=sum(B);

NSE=1-A2/B2;

%Relative Mean Error
for i=1:length(CGWR)
    if CGWR(i)~=0
    e(i)=(abs(TASGWR(i)- CGWR(i)))/CGWR(i);
    end
end
    E=sum(e);
    Err_rel=E/numel(CGWR);


% R2
Corr=corr2(TASGWR,CGWR)^2;

%Result Table
f=figure('Position', [300 500 700 160]);
title('Simulated and Calculated (Guttman&Zukerman) Total Annual Groundwater
Recharge - Efficiency')
cnames={'NSE','Err Rel','R^2'};
rnames={'value'};
tabella(:,1)=NSE;
tabella(:,2)=Err_rel;
tabella(:,3)=Corr;
t=uitable('Parent',f,'Data',tabella,'Position',[20 20 650
120],'ColumnName',cnames,'RowName',rnames);

%plot Annual Precipitation/theoretical GWR and weekly (or monthly)
Precipitation/ simulated GWR.

%plot Annual Precipitation and theoretical GWR
figure;
plot(TASR,CGWR,'.r')
title('Annual Precipitation and GWR after Guttman&Zukerman');
xlabel('Annual Precipitation (mm)');
ylabel('Annual GWR after Guttman&Zukerman (mm)');

%plot weekly Precipitation and simulated GWR
% weekly rain
SimRain2=SimRain;
SimRain2(3642:end)=[];
a=1;
for i=1:7:numel(SimRain2)
    if i<numel(SimRain2)
week_P(a)=sum(SimRain2(i:(i+7)));
a=a+1;
    end
end
%weekly GWR from the model
SimGWR2=SimGWR;
```

```
SimGWR2(3642:end)=[];
b=1;
for i=1:7:numel(SimGWR2)
    if i<numel(SimGWR2)
week_GWR(b)=sum(SimGWR2(i:(i+7)));
b=b+1;
    end
end
figure;
plot(week_P,week_GWR,'.b')
title('Weekly Precipitation and Simulated GWR by J2000g');
xlabel('Weekly Precipitation (mm)');
ylabel('Weekly GWR simlulated by J2000g (mm)');

%plot monthly Precipitation and simulated GWR

% monthly rain
SimRain2=SimRain;
SimRain2(3632:end)=[];
a=1;
for i=1:30:numel(SimRain2)
    if i<numel(SimRain2)
mont_P(a)=sum(SimRain2(i:(i+30)));
a=a+1;
    end
end
%monthly GWR from the model
SimGWR2=SimGWR;
SimGWR2(3632:end)=[];
b=1;
for i=1:30:numel(SimGWR2)
    if i<numel(SimGWR2)
mont_GWR(b)=sum(SimGWR2(i:(i+30)));
b=b+1;
    end
end
figure;
plot(mont_P,mont_GWR,'.b')
title('Monthly Precipitation and Simulated GWR by J2000g');
xlabel('Monthly Precipitation (mm)');
ylabel('Monthly GWR Simulated by J2000g (mm)');
```

A.6 Monthly Actual Evapotranspiration from different sources and Soil Moisture

Script compare simulated monthly actual evapotranspiration with AET from two different satellite database and monthly average soil moisture.

```
clc
clear all
close all

filename =
'Y:\Gruppen\na_osten\Alessandro\work\JAMS\AlessandroDarga\output\current\re
sult-gb.dat';
DELIMITER = '\t';
HEADERLINES = 3; %J2000g output

% Import the file
All = importdata(filename, DELIMITER, HEADERLINES);
% Read 1 column
AETJ2000g = All.data(:,13); %into the file result-gb the column n.13 is
                             %actET, the n.12 is potET
J=length(AETJ2000g);

MonthlyAET=xlsread('Y:\Gruppen\na_osten\Alessandro\work\JAMS\PET\scripts\Mo
nthlyET03-06');

% put each monthly value to all days of that month
a=1;
for i=1:numel(MonthlyAET)
    for j=1:30
    M_AET(a,:) = MonthlyAET(i);
    a=a+1;
    end
end

M=length(M_AET);

%transform daily simulated AET in monthly AET
AETJ2000g(3632:end)=[];
b=1;
for i=1:30:length(AETJ2000g)
     if i<numel(AETJ2000g)
    AETJ2(b)=sum(AETJ2000g(i:i+30));
    b=b+1;
     end
end

a=1;
for i=1:numel(AETJ2)
    for j=1:30          %writes 30-day entry to 30 single day entries
    AETJ2000g(a,:) = AETJ2(i);
    a=a+1;
```

```
    end
end

%vectors have to have same length, cut the longest
if M>J    %if M_AET has more values than AETJ2000g
M_AET(J+1:end)=[]; %delete surplus of values,
else
    AETJ2000g(M+1:end)=[];
end

t=1:min(M,J);
t=t';
T=length(t);
% Import Soil Moisture (ACTMPS-> actual middle sized pore storage)
SM = All.data(:,16); %import ACTMPS from result-gb
%SM = All.data(:,17); %import satMPS from result-gb --> relative soil
%moisture

% transform daily soil moisture in average monthly soil moisture
SM(3632:end)=[];
b=1;
for i=1:30:length(SM)
     if i<numel(SM)
    meanSM(b)=mean(SM(i:i+30));
    b=b+1;
     end
end

a=1;
for i=1:numel(meanSM)
    for j=1:30           %writes 30-day entry to 30 single day entries
    SM(a,:) = meanSM(i);
    a=a+1;
    end
end

H=length(SM);
if H>T % if SM has more values than the other two vectors
       %(AETJ2000g and AETmodis)
    SM(T+1:end)=[];
end
SM=SM';

%trasform Modis AET in monthly
load('AET_db8.mat');
AET(2552:end)=[];
b=1;
for i=1:30:length(AET)
     if i<numel(AET)
    AET2(b)=sum(AET(i:i+29));
    b=b+1;
     end
end

a=1;
```

```
for i=1:numel(AET2)
    for j=1:30           %writes 30-day entry to 30 single day entries
    AET(a,:) = AET2(i);
    a=a+1;
    end
end

K=length(AET);
if K>T % if SM has more values than the other two vectors
        %(AETJ2000g and AETmodis)
    AET(T+1:end)=[];
end

figure;
plot(t,M_AET,'-r',t,AET,'y',t,AETJ2000g,'-g',t,SM,'-b')
title('monthly satellite ET,monthly modis ET, monthly simulated ET and
monthly average Soil Moisture');
xlabel('Time (Days)');
ylabel('AET');
legend('AET by Zhang et al','Modis ET','Model AET','average Soil Moisture')

figure;
plot(t,M_AET,'-r',t,AET,'b',t,AETJ2000g,'-g')
title('monthly ET by Zhang et al, monthly Modis ET, monthly simulated ET');
xlabel('Time (Days)');
ylabel('AET (mm)');
legend('AET by Zhang et al','Modis AET','Model AET')
```

A.7 Runoff comparison

Script calculates in which days there are available discharge data and compares in this days model's response with measured values. Comparison is done with and without a threshold of tolerance.

```
%Runoff comparison
clc
clear all
close all
filename =
'Y:\Gruppen\na_osten\Alessandro\work\JAMS\AlessandroDarga\output\current\ru
noff_out.dat';
DELIMITER = '\t';
HEADERLINES = 3;

% Import the file
All = importdata(filename, DELIMITER, HEADERLINES);
% Read 1 column
SimRoff = All.data(:,1); %read dirQ. choose 2 for basQ and 3 for totQcbm
n=numel(SimRoff);

filename =
'Y:\Gruppen\na_osten\Alessandro\work\JAMS\AlessandroDarga\data\orun.dat';
DELIMITER = '\t';
HEADERLINES = 16;

% Import the file
All = importdata(filename, DELIMITER, HEADERLINES);
% Read 1 column
ObsRoff = All.data(:,1); %read observated runoff darga
l=length(ObsRoff);

OR=ObsRoff(ObsRoff~=-9999);
position=find(ObsRoff~=-9999);
SR=SimRoff(position);
days_with_values=numel(OR) %count how many values with measures there are
in Obsrunoff Darga

%count how many days, from ones with measures, model can predict
a=0;
b=0;
c=0;
d=0;
for i=1:n
    if SimRoff(i)==0 && ObsRoff(i)==0
        c=c+1;
    end
end

for i=1:n
```

```
    if SimRoff(i)~=0 && ObsRoff(i)~=-9999 && ObsRoff(i)~=0
        b=b+1;

    end
end
predicted_values =c+b

%count how many days, from ones with measures, model can predict with
%a precise tolerance

p=0.5;  %tolerance: can vary between 0 and 1
Tolerance_percentage=p
z=0;
for j=1:length(OR)
    if OR(j)==0
        z=z+1;
        if SR(j)<=0.3
            a=a+1;
        end
    end
end
w=0;
for j=1:length(OR)
    if OR(j)~=0
        w=w+1;
        mi(j)=OR(j)-(OR(j)*p);
        ma(j)=OR(j)+(OR(j)*p);
            if SR(j)<=ma(j)
                if SR(j)>=mi(j)
                d=d+1;
                end
            end
    end
end

predicted_values_with_tolerance_p =a+d


%Nash-Sutcliffe efficiency NSE

MeanOR=mean(OR); %average value of the vector OR

for i=1:length(OR)
    A(i)=(SR(i)-OR(i))^2;

    B(i)=(OR(i)-MeanOR)^2;

end
A2=sum(A);
B2=sum(B);
NSE=1-A2/B2;

%Relative Mean Error
```

```
for i=1:length(OR)
    if OR(i)~=0
    e(i)=(abs(SR(i)- OR(i)))/OR(i);
    end
end
    E=sum(e);
    Err_rel=E/numel(OR);


% R2

Corr=corr2(OR,SR)^2;

%Result Table

f=figure('Position', [300 500 700 160]);
title('Efficiency in the prediction of Runoff')
cnames={'NSE','Err Rel','R^2'};
rnames={'value'};
tabella(:,1)=NSE;
tabella(:,2)=Err_rel;
tabella(:,3)=Corr;
t=uitable('Parent',f,'Data',tabella,'Position',[20 20 650
120],'ColumnName',cnames,'RowName',rnames);
```

A.8 Soil Moisture

Script plots absolute and relative Soil Moisture against time.

```
%Soil Moisture plotting
clc
clear all
close all

filename =
'Y:\Gruppen\na_osten\Alessandro\work\JAMS\AlessandroDarga\output\current\re
sult-gb.dat';
DELIMITER = '\t';
HEADERLINES = 3; %J2000g output

% Import the file
All = importdata(filename, DELIMITER, HEADERLINES);
% Read 1 column
relSoilM = All.data(:,17); %column 17 satMPS --> relative soil moisture
AbsSoilM = All.data(:,16); %column 16 actMPS --> absolute soil moisture
L=length(relSoilM);
T=1:L;

figure;
plot(T,relSoilM,'b')
title('relative Soil Moisture');
xlabel('Time (Days)');
ylabel('%');


figure;
plot(T,AbsSoilM,'r')
title('Absolute Soil Moisture');
xlabel('Time (Days)');
ylabel('mm');
```

A.9 Temperature

Script plots mean temperature (Celsius Degree) against time.

```
%Temperature plotting

Tmean = All.data(:,2);  %read the column Tmean from result-gb
t=1:numel(Tmean);
figure
plot(t,Tmean, 'r')
title('Average daily temperature');
xlabel('Time (Days)');
ylabel('Celsius degree');
```

REFERENCES

Al-Qurashi A. (2008): Apllication of the kineros2 rainfall-runoff model to an arid catchment in Oman

Arkin Y. (2007): Geotechnical and Hydrogeological Concerns in Developing the Infrastructure around Jerusalem

Bahat Y. (2009): Rainfall-runoff modeling in a small hyper-arid catchment

BasimDudeen (2001): The Soils of Palestine (the West Bank and Gaza Strip) Current Status and Future Perspective

Beven K. (2001): Rainfall-runoff modelling

Dan J. (1963): the soils of Israel and their distribution

Dan J. (1983): Soil Chronosequences in Israel

Dan, J. (1972): The Soil association map of Israel

Dan, J. (1976): Soils of Israel

Garcia-Pintado J. (2009): Calibration of structure in a distributed forecasting model for a semiarid flash flood: Dynamic surface storage and channel roughness

Guttman J. & Zukerman H. (1995): Flow Model in the Eastern Basin of the Judea and Samaria Hills.

Hasan J. (2009): Nature and the Origin of EinFeshcha Springs

Hogan M. (2010): Climate tends in Israel over a 30 year period

Hoshin V. (2009): Decomposition of the mean squared error and NSE performance criteria: Inplication for improving hydrological modeling

http://www.era-envhealth.eu

Jamswiki (2010): http://jams.uni-jena.de

Knoche M. (2010): Water balance of the upper Awash catchment, estimated using remote sensing data implemented in the J2000g hydrological model

Knote C. (2009): Leaf Area Index Specification for Use in Mesoscale Weather Prediction System

Krause P. (2009): Simulation and analysis of the impact of projected climate change on the spatially distributed waterbalance in Thuringia, Germany

Kumar R. (2010): The effects of spatial discretization and model parameterization on the prediction of extreme runoff characteristics

Kumar R. (2012): Implications of distributed hydrologic model parameterization on water fluxes at multiple scales and locations

Marei A. (2010): Estimating groundwater recharge using the chloride mass-balance method in the West Bank, Palestine

Montanari A., Castellarin A. (2013): Corso di Modellistica Idrologica: Appunti dalle Lezioni, dispense dalle Modellistica Idrologica.

Monteith, J.L. (1965): Evaporation and environment.

Penman, H.L. (1948): Natural evaporation from open water, bare soil, and grass.

Reinfenberg, A. (1947): The soils of Palestine

Rödiger T. (2008): Multi-response calibration of a conceptual hydrological model in the semiarid catchment of Wadi al Arab, Jordan

Samaniego L. (2004): Robust parametric models of runoff characteristics at the mesoscale

Samaniego L. (2010): Multiscale parameter regionalization of a grid-based hydrologic model at the mesoscale

Samaniego L. (2011): Prediction in a data-sparse region using a regionalized grid-based hydrologic model driven by remotely sensed data

Schaefli B. (2007): Do Nash values have values?

Schulz S. (2008): Application of the water balance model J2000 to estimate groundwater recharge in a semi-arid environment – a case of study in the Zarqa River catchment, NW-Jordan

Seibert J. (2009): Gauging the ungauged basin: how many discharge measurement are needed?

Singer, A. (2007): The Soils of Israel

Sivapalan M. (2010): IAHS Decade on Prediction in Ungauged Basin (PUB), 2003-2012: Shaping an exiting future for the hydrological sciences

Terry, A. (2004): The Penman-Monteith method.

The Food and Agriculture Organization of the United Nations (1989): The arid environments.

Warren B. (2003): Comparisons of land cover and LAI estimates derived from ETM+ and MODIS for four sites in North America: a quality assessment of 2000/2001 provisional MODIS products

Wheater H. (2005): Modelling Hydrological Processes in Arid and Semi Arid Areas

www.fao.org - FAO Penman-Monteith equation

Zhang K. (2010): A continuous satellite-derived global record of land evapotranspiration from 1983-2006